EUROPEAN ORGANIZATION FOR NUCLEAR RESEARCH

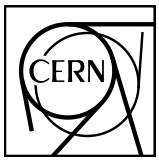

ALICE-PUBLIC-2018-011

Centrality determination in heavy ion collisions

ALICE Collaboration*

Abstract

This document describes the methods used by ALICE for the centrality determination. Specifically it addresses the modifications implemented with respect to previous publications [1, 2], which stems for:

- and a modification of the definition of the centrality classes, now defined according to the simulated multiplicity distribution;
- an update of the cross-section values used for the Glauber-MC calculations;
- a modification in the parameterization of the nuclear density charge which uses a weigthed sum of individual 2pF distributions for the proton and for the neutron;
- a uniform three-dimensional lattice to parameterize the minimum nodal separation between nucleons;
- the total systematic uncertainty obtained by adding in quadrature the maximum/average of the up and downward variations from all sources.

*See Appendix A for the list of collaboration members

1 Introduction

The centrality is defined as the percentile of the hadronic cross section corresponding to a particle multiplicity, or an energy deposited, measured in ALICE, above a given threshold (N_{ch}^{THR})

$$c \approx \frac{1}{\sigma_{AA}} \int_{N_{ch}^{THR}}^{\infty} \frac{\mathrm{d}\sigma}{\mathrm{d}N'_{\mathrm{ch}}} \mathrm{d}N'_{\mathrm{ch}} \approx \frac{1}{\sigma_{AA}} \int_{0}^{E_{ZDC}^{THR}} \frac{\mathrm{d}\sigma}{\mathrm{d}E'_{ZDC}} \mathrm{d}E'_{ZDC}. \tag{1}$$

The Glauber model is widely used to describe the dependence of N_{part} and N_{coll} on b in p–A, d–A and A–A collisions [3–6]. The purpose of Monte Carlo implementations of the Glauber model [7, 8] is to compose two nuclei out of nucleons and simulate their collision process event-by-event. Geometrical quantities are calculated by simulating many nucleus-nucleus collisions. Coupling the Glauber MC to a model of particle production, one can calculate the produced particle multiplicity distribution that can be compared to the experimentally measured one. Mean values of geometrical quantities are then calculated for centrality classes defined by classifying the events according to their multiplicity.

This documents presents the ALICE methods for the centrality determination, focussing to the changes introduced with respect to the past [1], i.e. a modification of the definition of the centrality classes, now defined according to the simulated multiplicity distribution, an update of the cross-section values used for the Glauber-MC calculations, as well as a modification in the parameterization of the nuclear density charge which uses a weigthed sum of individual 2pF distributions for the proton and for the neutron, and a uniform three-dimensional lattice to parameterize the minimum nodal separation between nucleons. Finally the total systematic uncertainty obtained by adding in quadrature the maximum/average of the up and downward variations from all sources. Section 2 summarizes the methods for the Glauber-MC and the NBD-Glauber fot to the multiplicity distribution. Section 4 and Section 3 provide tables with calculated quantities for Pb–Pb collisions at $\sqrt{s_{\mathrm{NN}}}$ = 2.76 and 5.02 TeV, and the differences with previously used values. Section 5 provides the values for the Xe–Xe collisions at $\sqrt{s_{\mathrm{NN}}}$ = 5.44 TeV.

2 The Glauber Monte Carlo

2.1 The nucelar charge distribution

Following [9], the first step in the Glauber Monte Carlo is to prepare a model of the two nuclei by defining stochastically the position of the nucleons in each nucleus. The nucleon position in the ^{208}Pb nucleus is determined by the nuclear density function, modeled by the functional form (modified Woods-Saxon or 2-parameter Fermi distribution):

$$\rho(r) = \rho_0 \frac{1 + w(r/R)^2}{1 + \exp\left(\frac{r-R}{a}\right)} \tag{2}$$

The parameters are based on data from low energy electron-nucleus scattering experiments [10]. Protons and neutrons are assumed to have the same nuclear profile. The parameter ρ_0 is the nucleon density, which provides the overall normalization, not relevant for the Monte Carlo simulation, R is the radius parameter of the ^{208}Pb nucleus and a is the skin thickness of the nucleus, which indicates how quickly the nuclear density falls off near the edge of the nucleus. The additional parameter w is needed to describe nuclei whose maximum density is reached at radii $r > 0$ ($w = 0$ for Pb). According to [11] we used a weigthed sum of individual 2pF distributions for the proton and for the neutron with $R_p = 6.68 \pm 0.02$ and $a_p = 0.447 \pm 0.01$, $R_n = 6.69 \pm 0.03$ and $a_n = 0.560 \pm 0.03$. In the Monte Carlo procedure the radial coordinate of a nucleon is randomly drawn from the distribution $4\pi r^2 \rho(r)$ and ρ_0 is determined by the overall normalization condition $\int \rho(r) d^3 r = A$. Instead of the hard-sphere exclusion distance previously used ($d_{\mathrm{min}} = (0.4 \pm 0.4)$ fm), we employ a uniform three-dimensional lattice with a minimum nodal separation (d_{node}) equivalent to d_{min}. It is equivalently treated with a variation of 100%, $d_{\mathrm{node}} = (0.4 \pm 0.4)$ fm.

2.2 The nucleon-nucleon cross-section

The second step is to simulate a nuclear collision. The impact parameter b is randomly selected from the geometrical distribution $dP/db \sim b$ up to a maximum $b_{\max} \simeq 20\,\mathrm{fm} > 2R_{\mathrm{Pb}}$, large enough to simulate collisions until the interaction probability becomes zero. The nucleus-nucleus collision is treated as a sequence of independent binary nucleon-nucleon collisions, where the nucleons travel on straight-line trajectories and the inelastic nucleon-nucleon cross section is assumed to be independent of the number of collisions a nucleon underwent previously, i.e. the same cross section is used for all successive collisions. Two nucleons from different nuclei are assumed to collide if the relative transverse distance between centers is less than the distance corresponding to the inelastic nucleon-nucleon cross section $d < \sqrt{\sigma_{\mathrm{NN}}^{\mathrm{inel}}/\pi}$.

The value of the cross-section $\sigma_{\mathrm{NN}}^{\mathrm{inel}}$ is typically estimated by interpolation of pp data at different center-of-mass energies and from cosmic rays, and subtracting the elastic scattering cross section from the total cross section. According to [11], we decided to adopt:

- $\sqrt{s_{\mathrm{NN}}} = 2.76$ TeV: $\sigma_{\mathrm{NN}}^{\mathrm{inel}} = 61.8 \pm 0.9$ mb.
- $\sqrt{s_{\mathrm{NN}}} = 5.02$ TeV: $\sigma_{\mathrm{NN}}^{\mathrm{inel}} = 67.6 \pm 0.6$ mb.
- $\sqrt{s_{\mathrm{NN}}} = 5.44$ TeV: $\sigma_{\mathrm{NN}}^{\mathrm{inel}} = 68.4 \pm 0.5$ mb.
- $\sqrt{s_{\mathrm{NN}}} = 8.16$ TeV: $\sigma_{\mathrm{NN}}^{\mathrm{inel}} = 72.5 \pm 0.5$ mb.

in contrast to the previously used values: $\sqrt{s_{\mathrm{NN}}} = 2.76$ TeV: $\sigma_{\mathrm{NN}}^{\mathrm{inel}} = 64 \pm 5$ mb [1]; $\sqrt{s_{\mathrm{NN}}} = 5.02$ TeV: $\sigma_{\mathrm{NN}}^{\mathrm{inel}} = 70 \pm 5$ mb [2].

The number of collisions N_{coll} and the number of participants N_{part} are determined by counting, respectively, the binary nucleon collisions and the nucleons that experience at least one collision. Following the notation in [3], the geometric nuclear overlap function T_{PbPb} is then calculated as $T_{\mathrm{PbPb}} = N_{\mathrm{coll}}/\sigma_{\mathrm{NN}}^{\mathrm{inel}}$, and represents the effective nucleon luminosity in the collision process.

The total Pb–Pb cross section is calculated as $\sigma_{\mathrm{PbPb}} = N_{\mathrm{evt}}(N_{\mathrm{coll}} \geq 1)/N_{\mathrm{evt}}(N_{\mathrm{coll}} \geq 0) \times \pi b_{\mathrm{max}}^2$, i.e. the geometrical value corrected by the fraction of events with at least one nucleon-nucleon collision. It amounts to

- $\sigma_{\mathrm{PbPb}} = (7.67 \pm 0.16(syst.))$ b for Pb–Pb at 5.02 TeV,
- $\sigma_{\mathrm{PbPb}} = (7.55 \pm 0.12(syst.))$ b for Pb–Pb at 2.76 TeV,
- $\sigma_{\mathrm{pPb}} = (2.10 \pm 0.055(syst.))$ b for p–Pb at 5.02 TeV,
- $\sigma_{\mathrm{pPb}} = (2.12 \pm 0.047(syst.))$ b for p–Pb at 8.16 TeV,
- $\sigma_{\mathrm{XeXe}} = (5.7 \pm 0.2(syst.))$ b for Xe–Xe at 5.44 TeV.

2.3 The NBD-Glauber fit to the multiplicity distribution

To reproduce the experimental multiplicity distribution, the Glauber Monte Carlois coupled to a model for particle production, based on a negative binomial distribution (NBD). This use of NBD is motivated by the fact that in minimum bias pp and $\mathrm{p\overline{p}}$ collisions at high energy, the charged particle multiplicity $d\sigma/dN_{\mathrm{ch}}$ has been measured over a wide range of rapidity and is well described by a NBD [12, 13].

The Glauber Monte Carlo defines, for an event with a given impact parameter b, the corresponding N_{part} and N_{coll}. The particle multiplicity per nucleon-nucleon collision is parametrized by a NBD. To apply

this model to any collision with a given $N_{\rm part}$ and $N_{\rm coll}$ value we introduce the concept of "ancestors", i.e. independently emitting sources of particles. We assume that the number of ancestors $N_{\rm ancestors}$ can be parameterized by $N_{\rm ancestors} = f \cdot N_{\rm part} + (1-f) \cdot N_{\rm coll}$. This is inspired by two-component models [14, 15], which decompose nucleus–nucleus collisions into soft and hard interactions, where the soft interactions produce particles with an average multiplicity proportional to $N_{\rm part}$, and the probability for hard interactions to occur is proportional to $N_{\rm coll}$.

To generate the number of particles produced per interaction, we use the negative binomial distribution

$$P_{\mu,k}(n) = \frac{\Gamma(n+k)}{\Gamma(n+1)\Gamma(k)} \cdot \frac{(\mu/k)^n}{(\mu/k+1)^{n+k}}, \tag{3}$$

which gives the probability of measuring n hits per ancestor, where μ is the mean multiplicity per ancestor and k controls the width. For every Glauber Monte Carlo event, the NBD is sampled $N_{\rm ancestors}$ times to obtain the averaged simulated VZERO amplitude for this event, which is proportional to the number of particles hitting the hodoscopes. The VZERO amplitude distribution is simulated for an ensemble of events and for various values of the NBD parameters μ, k, and the $N_{\rm ancestors}$ parameter f. A minimization procedure is applied to find the parameters which result in the smallest χ^2. The fit is performed for VZERO amplitudes large enough so that the purity of the event sample and the efficiency of the event selection is 100%. That leaves a very broad range in the amplitude values that can be fitted to extract parameters f, μ and k directly from the data. The quality of the fit is good, as the χ^2/NDF is approximately unity for all fits. However we note that the high multiplicity tail, which is quite sensitive to fluctuations and the detector resolution not implemented in the model, is not perfectly well described.

We can then calculate the mean number of participants $\langle N_{\rm part}\rangle$ and collisions $\langle N_{\rm coll}\rangle$, and the mean nuclear thickness function $\langle T_{\rm PbPb}\rangle$ for centrality classes defined by sharp cuts in the simulated VZERO distribution. This is different to what was done in the past, where centrality classes were defined by cuts in the impact parameter. The root mean square (RMS) of these distributions is a measure for the magnitude of the dispersion of the quantities.

The systematic uncertainties on the mean values are obtained by independently varying the parameters of the Glauber model within their estimated uncertainties and repeating the fit for all the parameter variations. The total systematic uncertainty is obtained by adding in quadrature the maximum/average of the up and downward variations from all sources. Figure 1 shows the resulting variations for Pb–Pb collisions at $\sqrt{s_{\rm NN}}$= 5.02 TeV, for centrality classes defined by multiplicity or impact parameter, respectively.

3 Pb-Pb collisions at $\sqrt{s_{\rm NN}}$ = 5.02 TeV

Figure 2 shows the distribution of V0 amplitudes for all triggered Pb–Pb collisions at $\sqrt{s_{\rm NN}}$ = 5.02 TeV with a vertex within 10 cm, fitted by a Glauber-NBD fit.

Table 1 shows the geometric properties ($N_{\rm part}$, $N_{\rm coll}$, $T_{\rm PbPb}$) of Pb–Pb collisions at $\sqrt{s_{\rm NN}}$ = 5.02 TeV for centrality classes defined by sharp cuts in the V0M multiplicity distribution, simulated with an NBD-Glauber fit. The mean values, the RMS, and the systematic uncertainties are obtained with a Glauber Monte Carlo calculation.

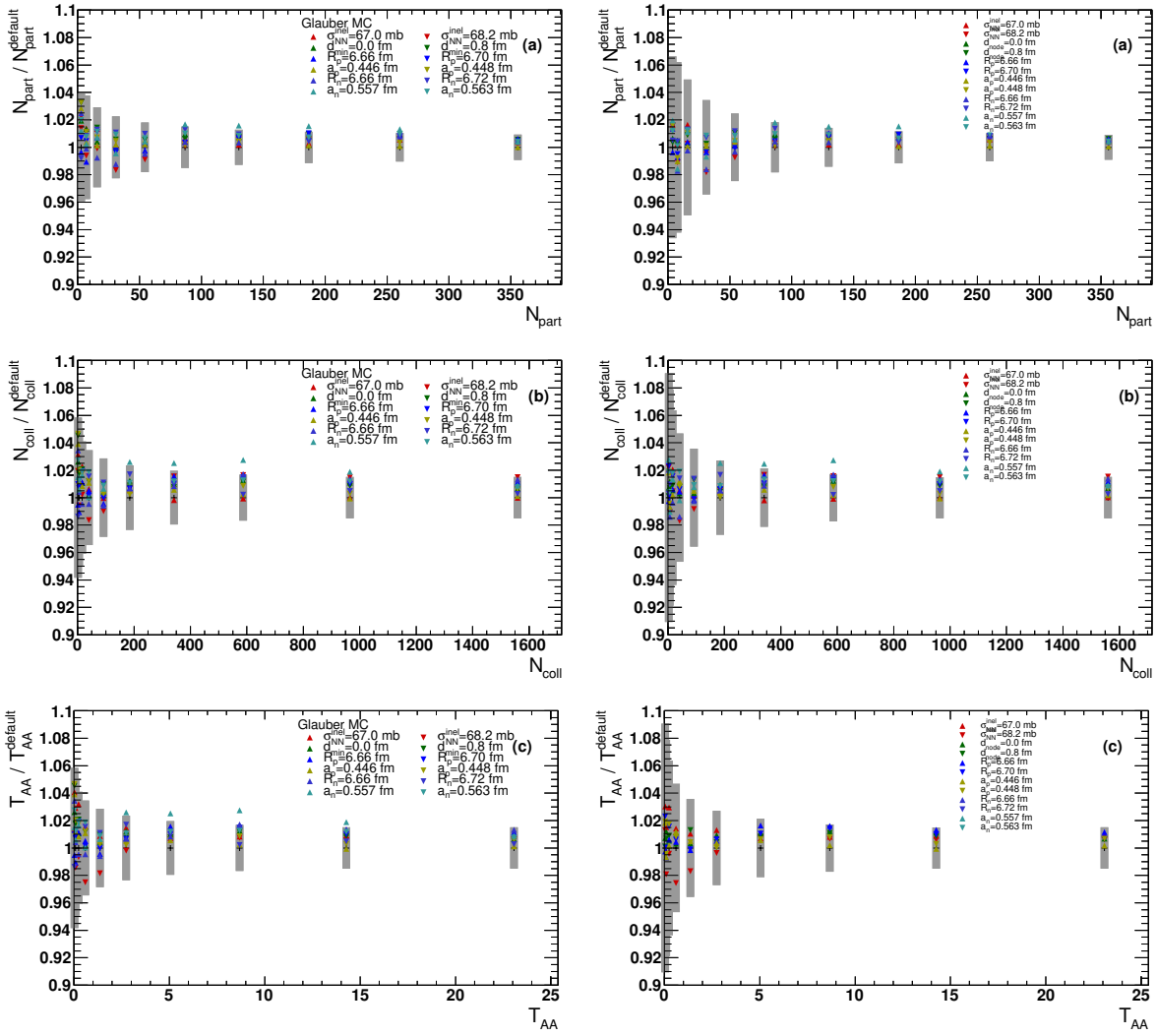

Fig. 1: Sensitivity of N_{part}, N_{coll}, and $T_{\mathrm{PbPb}}$to variations of parameters in the Glauber Monte Carlo model of Pb–Pb collisions at $\sqrt{s_{\mathrm{NN}}}$= 5.02 TeV for centrality classes defined by multiplicity (left) or impact parameter (right), respectively. The gray band represents the RMS scaled by a factor 0.1 for visibility.

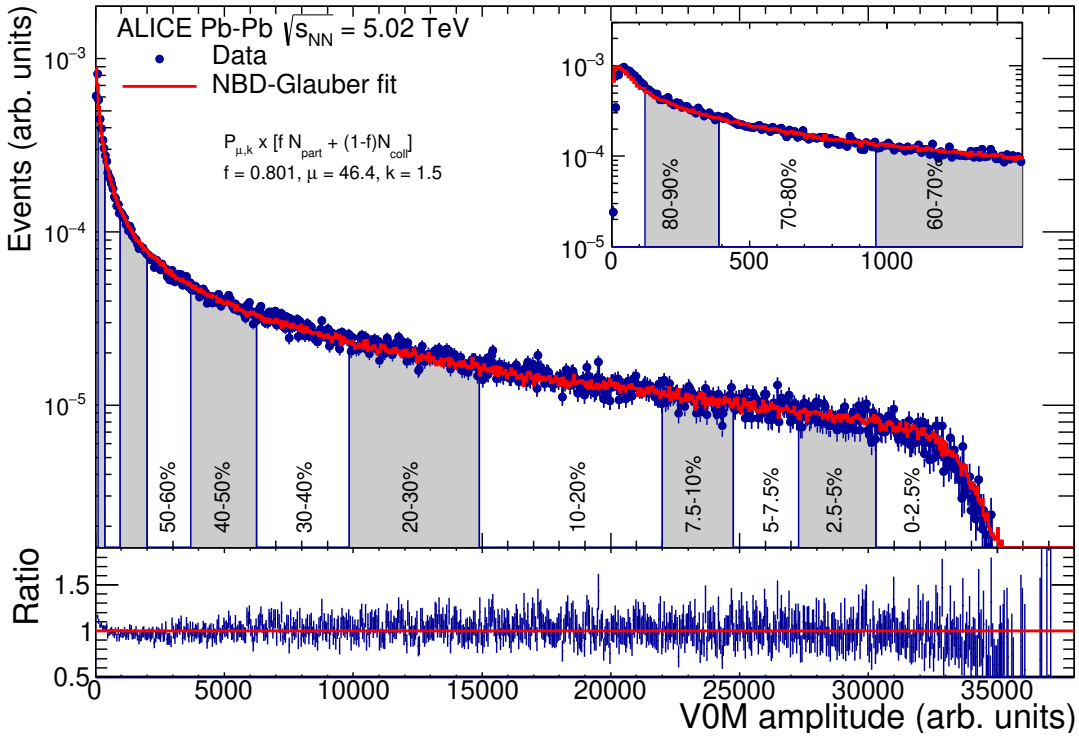

Fig. 2: Distribution of the sum of amplitudes in the V0 scintillators for Pb–Pb collisions at $\sqrt{s_{\rm NN}}$5.02 TeV. The distribution is fitted with the NBD-Glauber fit shown as a line. The inset shows a zoom of the most peripheral region.

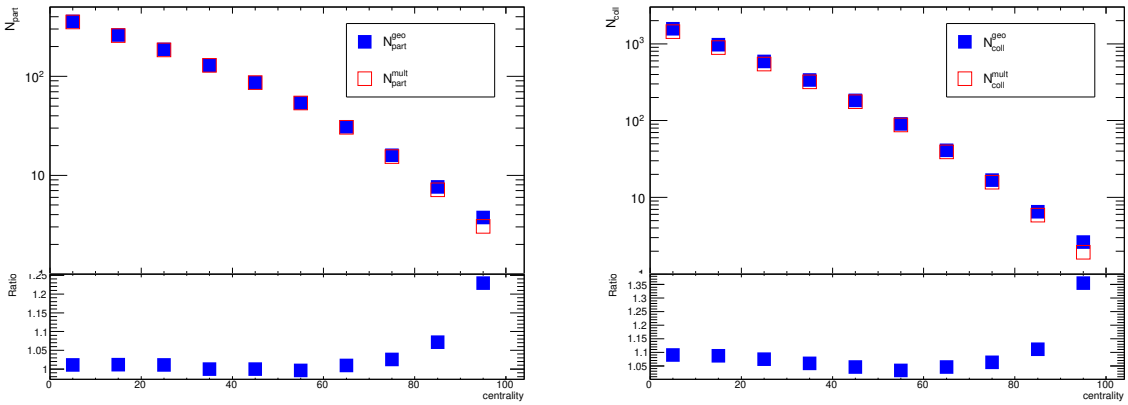

Fig. 3: Mean values of $N_{\rm part}$and $N_{\rm coll}$for centrality classes defined by multiplicity or impact parameter, respectively.

Table 1: Geometric properties ($N_{\rm part}$, $N_{\rm coll}$, $T_{\rm PbPb}$) of Pb–Pb collisions at $\sqrt{s_{\rm NN}}$ = 5.02 TeV for centrality classes defined by sharp cuts in the V0M multiplicity distribution, simulated with an NBD-Glauber fit. The mean values, the RMS, and the systematic uncertainties are obtained with a Glauber Monte Carlo calculation.

Centrality	$\langle N_{\rm part}\rangle$	RMS	(*sys.*)	$\langle N_{\rm coll}\rangle$	RMS	(*sys.*)	$\langle T_{\rm PbPb}\rangle$ (1/mbarn)	RMS (1/mbarn)	(*sys.*) (1/mbarn)
0-1%	401.9	7.55	0.46	1949	87	21.1	28.83	1.29	0.177
1-2%	393.9	10.2	0.496	1844	81.3	20.1	27.28	1.2	0.171
2-3%	384.4	11.7	0.752	1755	80.8	20.3	25.96	1.19	0.2
3-4%	373.9	12.5	0.762	1673	79.9	18.8	24.75	1.18	0.18
4-5%	362.9	13	0.738	1593	77.6	17.8	23.57	1.15	0.178
0-2.5 %	395.7	11.1	0.481	1872	107	20.4	27.69	1.58	0.175
2.5-5 %	371.1	14.5	0.738	1654	95.4	18.5	24.46	1.41	0.18
5-7.5 %	344	14.9	0.927	1464	88.1	16.8	21.66	1.3	0.174
7.5-10%	318.4	14.7	1.15	1300	81.7	14.8	19.23	1.21	0.16
0-5 %	383.4	17.8	0.568	1763	149	19.4	26.08	2.21	0.176
5-10 %	331.2	19.6	1.03	1382	118	15.7	20.44	1.75	0.166
10-15 %	283	18.1	1.13	1090	97.3	12.3	16.12	1.44	0.135
15-20 %	241	16.6	1.22	857.3	83.1	10.5	12.68	1.23	0.118
20-25 %	204.1	15.1	1.33	668.8	70.7	9.21	9.894	1.05	0.11
25-30 %	171.7	13.6	1.36	516.6	59.8	7.32	7.641	0.884	0.0942
30-35 %	143.2	12.3	1.49	393	50.7	6.51	5.814	0.75	0.0917
35-40 %	118.4	11	1.2	294.6	42.1	5.12	4.358	0.624	0.073
40-45 %	96.58	9.76	1.08	216.1	34.9	3.83	3.197	0.516	0.0554
45-50 %	77.68	8.6	0.793	155.2	27.9	2.91	2.296	0.413	0.0427
50-55 %	61.28	7.49	0.9	108.6	21.8	2.61	1.607	0.323	0.0378
55-60 %	47.39	6.49	0.753	74.14	16.8	1.74	1.097	0.248	0.026
60-65 %	35.7	5.53	0.734	49.18	12.4	1.37	0.7275	0.184	0.0207
65-70 %	26.23	4.66	0.448	31.81	8.85	0.763	0.4706	0.131	0.012
70-75 %	18.63	3.9	0.329	20	6.27	0.502	0.2959	0.0927	0.0079
75-80 %	12.8	3.14	0.205	12.23	4.27	0.253	0.1808	0.0632	0.0041
80-85 %	8.481	2.45	0.171	7.198	2.81	0.236	0.1065	0.0416	0.0037
85-90 %	5.433	1.83	0.0625	4.104	1.84	0.0635	0.06071	0.0272	0.00126
90-95 %	3.309	1.22	0.0902	2.172	1.11	0.0844	0.03213	0.0165	0.00132
95-100 %	2.241	0.536	0.0441	1.228	0.497	0.0416	0.01816	0.00735	0.000673
0-10 %	357.3	32.1	0.753	1572	233	17.4	23.26	3.45	0.168
10-20 %	262	27.2	1.15	973.4	147	11.3	14.4	2.18	0.126
20-30 %	187.9	21.6	1.34	592.7	100	8.21	8.767	1.49	0.101
30-40 %	130.8	17	1.33	343.8	67.8	5.76	5.086	1	0.0814
40-50 %	87.14	13.2	0.928	185.7	43.9	3.33	2.747	0.649	0.0486
50-60 %	54.34	9.87	0.802	91.41	26	2.11	1.352	0.385	0.0309
60-70 %	30.97	6.97	0.57	40.5	13.9	1.03	0.5992	0.205	0.0158
70-80 %	15.72	4.58	0.241	16.12	6.62	0.341	0.2385	0.098	0.00552
80-90 %	6.973	2.64	0.0729	5.667	2.84	0.1	0.08383	0.042	0.00178
90-100 %	2.785	1.09	0.0497	1.708	0.986	0.0474	0.02527	0.0146	0.000777
0-20%	309.7	56.2	0.895	1273	357	14.1	18.83	5.29	0.142
20-40%	159.4	34.5	1.32	468.2	151	6.92	6.927	2.23	0.0909
40-60%	70.74	20.1	0.859	138.5	59.3	2.7	2.049	0.878	0.0394
60-80%	23.35	9.64	0.404	28.31	16.3	0.68	0.4188	0.241	0.0106
80-100%	4.883	2.91	0.0627	3.691	2.9	0.0761	0.0546	0.0429	0.00133
60-100%	14.12	11.7	0.255	16	17	0.409	0.2367	0.251	0.00637
0-30%	269.1	74.5	0.993	1046	437	11.7	15.48	6.47	0.121
30-50%	109	26.6	1.11	264.8	97.5	4.51	3.917	1.44	0.0645

4 Pb-Pb collisions at $\sqrt{s_{\rm NN}}$ = 2.76 TeV

Figure 4 shows the distribution of V0 amplitudes for all triggered Pb–Pb collisions at $\sqrt{s_{\rm NN}}$ = 2.76 TeV with a vertex within 10 cm, fitted by a Glauber-NBD fit.

Table 2 shows the geometric properties ($N_{\rm part}$, $N_{\rm coll}$, $T_{\rm PbPb}$) of Pb–Pb collisions at $\sqrt{s_{\rm NN}}$ = 2.76 TeV for centrality classes defined by sharp cuts in the V0M multiplicity distribution.

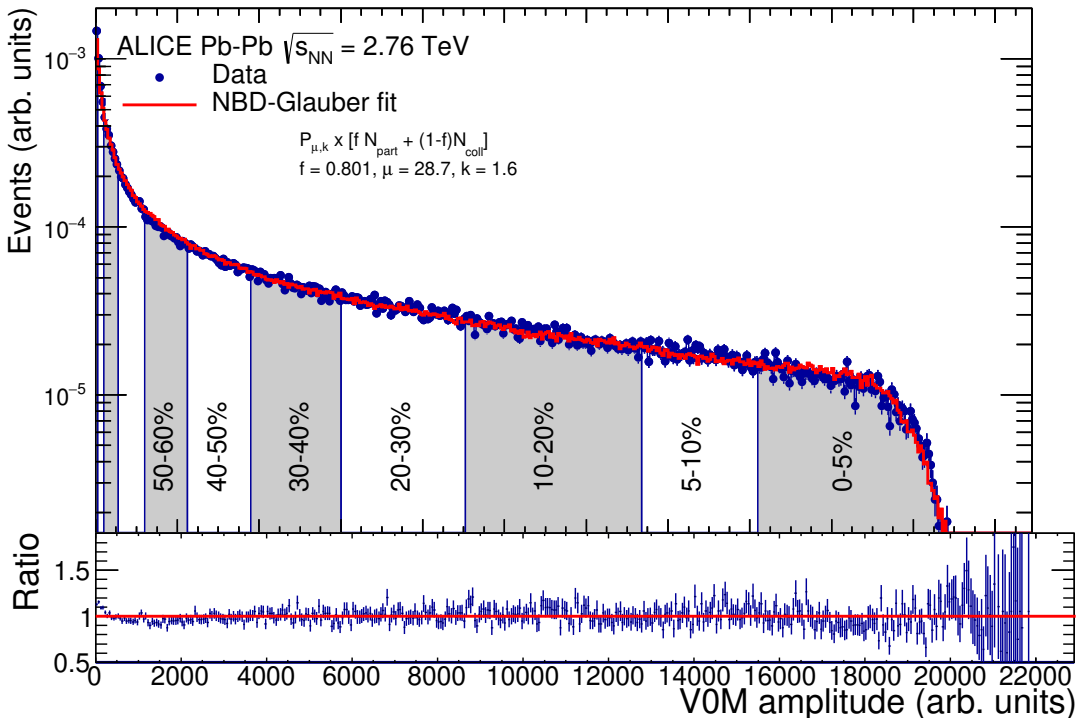

Fig. 4: Distribution of the sum of amplitudes in the V0 scintillators for Pb–Pb collisions at $\sqrt{s_{\rm NN}}$ 2.76 TeV. The distribution is fitted with the NBD-Glauber fit shown as a line.

Table 2: Geometric properties ($N_{\rm part}$, $N_{\rm coll}$, $T_{\rm PbPb}$) of Pb–Pb collisions at $\sqrt{s_{\rm NN}}$ = 2.76 TeV for centrality classes defined by sharp cuts in the V0M multiplicity distribution, simulated with an NBD-Glauber fit. The mean values, the RMS, and the systematic uncertainties are obtained with a Glauber Monte Carlo calculation.

Centrality	$\langle N_{\rm part}\rangle$	RMS	(*sys.*)	$\langle N_{\rm coll}\rangle$	RMS	(*sys.*)	$\langle T_{\rm PbPb}\rangle$ (1/mbarn)	RMS (1/mbarn)	(*sys.*) (1/mbarn)
0-1%	400.8	7.7	1.3	1788	79	32	28.94	1.3	0.29
1-2%	392.4	10	1.5	1694	76	32	27.42	1.2	0.26
2-3%	382.3	12	1.9	1614	76	32	26.11	1.2	0.29
3-4%	371.5	12	2.3	1537	73	33	24.86	1.2	0.31
4-5%	360.4	13	2.5	1464	72	31	23.68	1.2	0.27
0-2.5 %	394.2	11	1.2	1720	98	31	27.83	1.6	0.26
2.5-5 %	368.7	15	2.3	1519	88	32	24.58	1.4	0.29
5-7.5 %	341.2	15	2.6	1345	81	29	21.76	1.3	0.23
7.5-10%	314.5	15	3.5	1193	76	26	19.3	1.2	0.23
0-5 %	381.5	18	1.7	1619	1.4e+02	31	26.2	2.2	0.27
5-10 %	327.8	20	2.8	1269	1.1e+02	27	20.53	1.8	0.23
10-15 %	280.1	18	2.8	1004	89	24	16.25	1.4	0.23
15-20 %	238.5	16	2.6	791.1	76	19	12.8	1.2	0.18
20-25 %	202.1	15	2.5	622.3	64	16	10.07	1	0.16
25-30 %	170.8	13	2.6	485	56	14	7.848	0.91	0.19
30-35 %	142.7	12	2.7	370.7	47	10	5.998	0.76	0.15
35-40 %	117.6	11	1.9	279.4	40	9.2	4.521	0.65	0.14
40-45 %	96.09	9.5	2.3	204.7	32	6.5	3.313	0.52	0.088
45-50 %	77.27	8.4	1.8	148.4	26	5.7	2.401	0.42	0.082
50-55 %	61.08	7.3	1.8	104.4	21	4.2	1.69	0.33	0.06
55-60 %	47.47	6.3	2	71.98	16	3.8	1.165	0.25	0.056
60-65 %	35.76	5.5	1.5	48.15	12	2.9	0.7792	0.19	0.045
65-70 %	26.31	4.6	1.2	31.32	8.7	1.9	0.5067	0.14	0.031
70-75 %	18.67	3.8	0.79	19.69	6.1	0.97	0.3186	0.098	0.016
75-80 %	12.91	3.1	0.71	12.18	4.1	0.81	0.1972	0.066	0.013
80-85 %	8.588	2.4	0.49	7.244	2.8	0.48	0.1172	0.045	0.0078
85-90 %	5.438	1.8	0.17	4.075	1.8	0.16	0.06594	0.029	0.0028
90-95 %	3.315	1.2	0.13	2.173	1.1	0.11	0.03517	0.018	0.002
95-100 %	2.238	0.53	0.091	1.224	0.49	0.082	0.01981	0.008	0.0014
0-10 %	354.7	33	1.9	1444	2.1e+02	28	23.37	3.5	0.2
10-20 %	259.3	27	2.7	897.7	1.3e+02	21	14.53	2.2	0.2
20-30 %	186.5	21	2.4	553.7	91	14	8.96	1.5	0.17
30-40 %	130.1	17	2.2	325	63	9.7	5.259	1	0.14
40-50 %	86.69	13	2	176.6	41	6	2.857	0.66	0.084
50-60 %	54.28	9.6	1.9	88.21	24	4	1.427	0.4	0.058
60-70 %	31.04	6.9	1.3	39.74	13	2.4	0.6431	0.22	0.038
70-80 %	15.81	4.5	0.78	15.96	6.4	0.93	0.2582	0.1	0.015
80-90 %	7.011	2.6	0.33	5.657	2.8	0.31	0.09153	0.046	0.0051
90-100 %	2.788	1.1	0.12	1.709	0.97	0.099	0.02765	0.016	0.0018
0-20%	307	56	2.2	1171	3.3e+02	24	18.95	5.3	0.19
20-40%	158.3	34	2.2	439.3	1.4e+02	12	7.109	2.2	0.15
40-60%	70.49	20	2	132.4	55	4.9	2.143	0.9	0.07
60-80%	23.42	9.6	1	27.84	16	1.6	0.4505	0.26	0.026
80-100%	4.9	2.9	0.17	3.682	2.9	0.16	0.05959	0.047	0.0028
60-100%	14.17	12	0.55	15.78	17	0.85	0.2554	0.27	0.013
0-30%	266.8	74	2.1	965.2	4e+02	20	15.62	6.4	0.17
30-50%	108.4	26	2.1	250.8	91	7.7	4.058	1.5	0.11

5 Xe-Xe collisions at $\sqrt{s_{\rm NN}}$ = 5.44 TeV

In the Monte Carlo Glauber calculation, the nuclear density for ^{129}Xe, is described by a Woods-Saxon distribution for a deformed nucleus.

Figure 5 shows the distribution of V0 amplitudes for all triggered Xe–Xe collisions at $\sqrt{s_{\rm NN}}$ = 5.44 TeV with a vertex within 10 cm, fitted by a Glauber-NBD fit.

Table 3 shows the geometric properties ($N_{\rm part}$, $N_{\rm coll}$, $T_{\rm XeXe}$) of Xe–Xe collisions at $\sqrt{s_{\rm NN}}$ = 5.44 TeV for centrality classes defined by sharp cuts in the V0M multiplicity distribution.

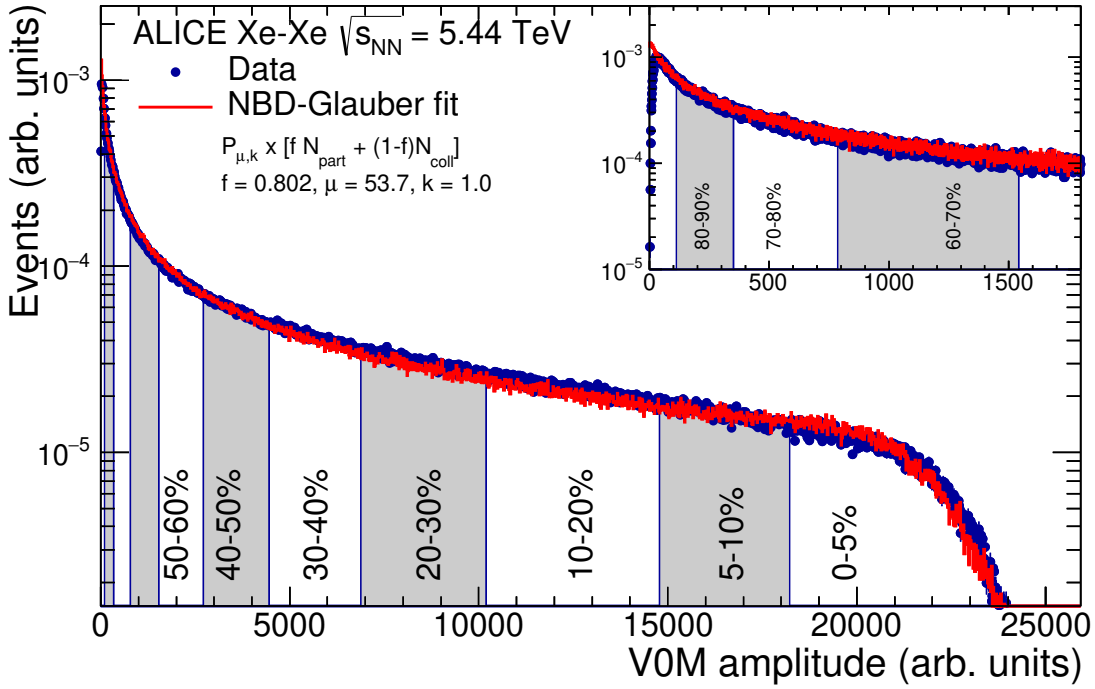

Fig. 5: Distribution of the sum of amplitudes in the V0 scintillators for Xe–Xe collisions at $\sqrt{s_{\rm NN}}$5.44 TeV. The distribution is fitted with the NBD-Glauber fit shown as a line. The inset shows a zoom of the most peripheral region.

Table 3: Geometric properties ($N_{\rm part}$, $N_{\rm coll}$, $T_{\rm PbPb}$) of Xe–Xe collisions at $\sqrt{s_{\rm NN}}$ = 5.44 TeV for centrality classes defined by sharp cuts in the V0M multiplicity distribution, simulated with an NBD-Glauber fit. The mean values, the RMS, and the systematic uncertainties are obtained with a Glauber Monte Carlo calculation.

Centrality	$\langle N_{\rm part}\rangle$	RMS	(*sys.*)	$\langle N_{\rm coll}\rangle$	RMS	(*sys.*)	$\langle T_{\rm XeXe}\rangle$ (1/mbarn)	RMS (1/mbarn)	(*sys.*) (1/mbarn)
0-2.5 %	242.3	7.7	1.3	1012	75	57	14.79	1.1	0.85
2.5-5 %	229.2	10	1.7	885.9	63	50	12.95	0.92	0.71
5-7.5 %	214.1	11	2.0	782.8	59	48	11.44	0.86	0.70
7.5-10%	199.2	11	1.8	691.8	55	45	10.11	0.81	0.65
0-5%	235.8	11	1.5	948.9	93	53	13.87	1.4	0.78
5-10%	206.7	13	1.8	737.3	73	46	10.78	1.1	0.67
10-15 %	177.8	13	1.6	574.7	62	37	8.402	0.91	0.54
15-20 %	151.8	12	2.4	446.4	52	35	6.527	0.76	0.51
20-25 %	128.7	11	2.6	343.8	44	31	5.026	0.65	0.45
25-30 %	108.2	9.7	2.7	261.7	38	26	3.826	0.55	0.39
30-35 %	90.14	8.7	2.7	196.7	31	21	2.876	0.45	0.31
35-40 %	74.26	7.8	2.7	145.9	25	17	2.134	0.37	0.25
40-45 %	60.48	6.9	2.5	106.7	20	13	1.56	0.3	0.19
45-50 %	48.63	6.0	2.5	76.87	16	10	1.124	0.24	0.15
50-55 %	38.36	5.3	2.3	54.25	13	7.1	0.7932	0.18	0.11
55-60 %	29.77	4.6	2.0	37.85	9.6	5.2	0.5534	0.14	0.078
60-65 %	22.63	3.9	1.6	25.89	7.2	3.5	0.3785	0.1	0.052
65-70 %	16.83	3.4	1.3	17.44	5.2	2.3	0.255	0.077	0.035
70-75 %	12.25	2.8	1.0	11.54	3.8	1.5	0.1687	0.055	0.021
75-80 %	8.741	2.3	0.65	7.502	2.7	0.85	0.1097	0.04	0.013
80-85 %	6.121	1.8	0.42	4.775	1.9	0.47	0.06981	0.028	0.0069
85-90 %	4.143	1.4	0.23	2.91	1.3	0.16	0.04255	0.019	0.0035
90-95 %	2.814	0.94	0.12	1.744	0.85	0.11	0.0255	0.012	0.0016
95-100 %	2.155	0.42	0.033	1.148	0.4	0.033	0.01679	0.0058	0.00049
0-10%	221.2	19	1.5	843.1	140	49	12.33	2	0.71
10-20 %	164.8	18	2.0	510.6	86	26	7.465	1.3	0.52
20-30 %	118.4	14	2.7	302.8	58	28	4.426	0.85	0.42
30-40 %	82.21	11	2.8	171.3	38	19	2.505	0.56	0.28
40-50 %	54.56	8.8	2.5	91.81	24	11	1.342	0.35	0.17
50-60 %	34.06	6.5	2.1	46.04	14	6.2	0.6731	0.2	0.091
60-70 %	19.72	4.7	1.5	21.65	7.6	2.9	0.3166	0.11	0.043
70-80 %	10.5	3.1	0.78	9.515	3.9	1.1	0.1391	0.056	0.017
80-90 %	5.127	1.9	0.33	3.838	1.9	0.35	0.05611	0.028	0.0052
90-100 %	2.488	0.8	0.085	1.449	0.73	0.071	0.02118	0.011	0.0011
0–20%	193	34	1.8	676.9	2e+02	42	9.896	2.9	0.62
20–90%	46.42	39	1.8	92.51	1.1e+02	10	1.352	1.5	0.14

Centrality	$\langle N_{\rm part}^{\rm geo}\rangle$	$\langle N_{\rm part}^{\rm mult}\rangle$	$\langle N_{\rm part}^{\rm geo}\rangle/\langle N_{\rm part}^{\rm mult}\rangle$	$\langle N_{\rm coll}^{\rm geo}\rangle$	$\langle N_{\rm coll}^{\rm mult}\rangle$	$\langle N_{\rm coll}^{\rm geo}\rangle/\langle N_{\rm coll}^{\rm mult}\rangle$	$\langle T_{\rm PbPb}^{\rm geo}\rangle$	$\langle T_{\rm PbPb}^{\rm mult}\rangle$	$\langle T_{\rm PbPb}^{\rm geo}\rangle/\langle T_{\rm PbPb}^{\rm mult}\rangle$
0-2.5%	244 ± 1.3	242.3 ± 1.3	1.00702	1010± 59	1012 ± 57	0.998024	14.8 ± 0.85	14.79 ± 0.84	1.00068
2.5-5%	229 ± 1.8	229.2 ± 1.7	0.999127	888 ± 54	885.9 ± 50	1.00237	13 ± 0.78	12.95 ± 0.71	1.00386
5-7.5%	214 ± 1.9	214.1 ± 2.0	0.999533	784 ± 50	782.8 ± 48	1.00153	11.5 ± 0.71	11.44 ± 0.70	1.00524
7.5-10%	199 ± 2.0	199.2 ± 2.8	0.998996	692 ± 46	691.8 ± 45	1.00029	10.1 ± 0.66	10.11 ± 0.65	0.999011
10-20%	164 ± 2.2	164.8 ± 2.0	0.995146	509 ± 37	510.6 ± 26	0.996866	7.45 ± 0.54	7.465 ± 0.52	0.997991
20-30%	118 ± 2.5	118.4 ± 2.7	0.996622	301 ± 28	302.8 ± 28	0.994055	4.4 ± 0.39	4.426 ± 0.42	0.994126
30-40%	81.5± 2.5	82.21 ± 2.8	0.991364	170 ± 18	171.3 ± 19	0.992411	2.49 ± 0.26	2.505 ± 0.28	0.994012
40-50%	54 ± 2.5	54.56 ± 2.5	0.989736	91.6± 11	91.81 ± 11	0.997713	1.34 ± 0.16	1.342 ± 0.17	0.99851
50-60%	33.7± 2.0	34.06 ± 2.1	0.98943	46.5± 6.3	46.04 ± 6.2	1.00999	0.68 ± 0.092	0.6731 ± 0.091	1.01025
60-70%	19.8± 1.4	19.72 ± 1.5	1.00406	22.4± 3.1	21.65 ± 2.9	1.03464	0.328 ± 0.045	0.3166 ± 0.043	1.03601
70-80%	11 ± 0.71	10.5 ± 0.78	1.04762	10.5± 1.2	9.515 ± 1.1	1.10352	0.154 ± 0.018	0.1391 ± 0.017	1.10712
80-90%	6.28± 0.32	5.127 ± 0.33	1.22489	5.12± 0.43	3.838 ± 0.35	1.33403	0.0749± 0.0064	0.05611 ± 0.0052	1.33488
90-100%	3.55± 0.01	2.488 ± 0.085	1.42685	2.44± 0.11	1.449 ± 0.071	1.68392	0.0357± 0.0016	0.02118 ± 0.0011	1.68555

6 p-Pb collisions at $\sqrt{s_{\rm NN}}$ = 8.16 TeV

Figure 6 shows the distribution of V0A amplitudes for all triggered p–Pb collisions with a vertex within 10 cm, fitted by a Glauber-NBD fit.

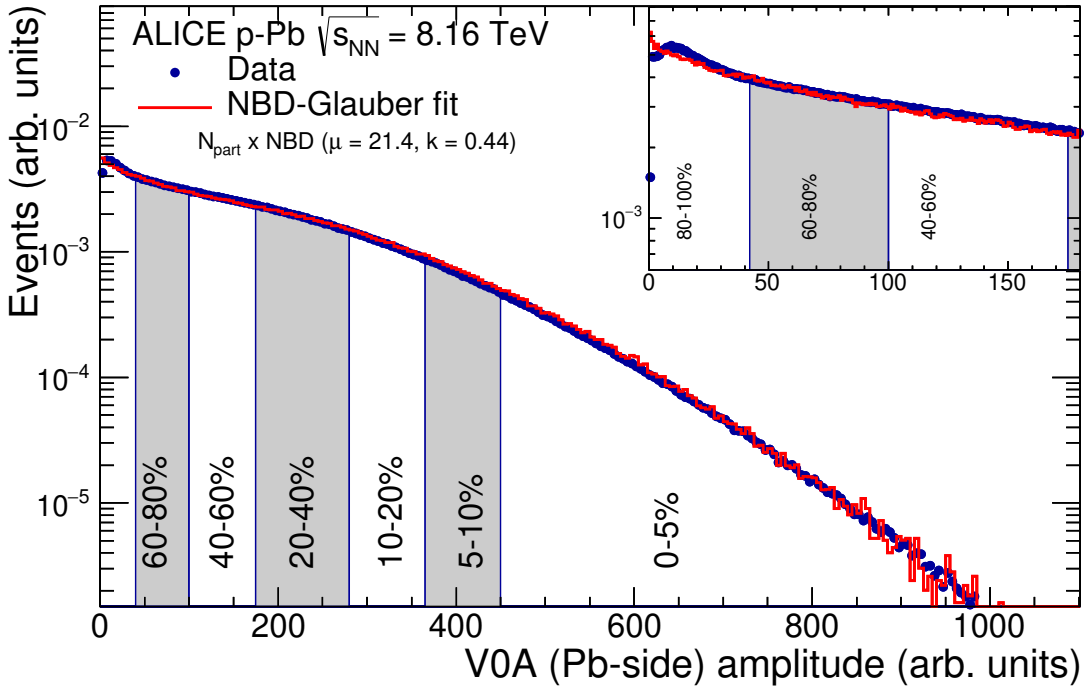

Fig. 6: Distribution of the sum of amplitudes in the V0A scintillators for p–Pb collisions at $\sqrt{s_{\rm NN}}$8.16 TeV. The distribution is fitted with the NBD-Glauber fit shown as a line. The inset shows a zoom of the most peripheral region.

Table 4 shows the geometric properties ($N_{\rm part}$, $N_{\rm coll}$, $T_{\rm pPb}$) of p–Pb collisions at $\sqrt{s_{\rm NN}}$ = 8.16 TeV for centrality classes defined by sharp cuts in the V0A, V0M or CL1 multiplicity distribution, simulated with an NBD-Glauber fit. The mean values, the RMS, and the systematic uncertainties are obtained with a Glauber Monte Carlo calculation.

As describedd in [2], the hybrid method aims to provide an unbiased centrality estimator. It is based on two assumptions, the first is that the event selection based on the energy deposited in the ZDC is free from the biases due to a multiplicity selection. The second assumption is that some observables scale linearly with $N_{\rm coll}$ and $N_{\rm part}$, allowing one to establish a relationship to the collision geometry. Two sets of $\langle N_{\rm coll}\rangle$ are calculated: $\langle N_{\rm coll}^{\rm mult}\rangle$ and $\langle N_{\rm coll}^{\rm Pb-side}\rangle$ for each centrality bin i estimated using the energy deposited in the neutron calorimeter on the Pb-going side (ZN). The first set is computed assuming that the charged-particle multiplicity at mid-rapidity is proportional to the $N_{\rm part}$. The second set is calculated using the Pb-side multiplicity. A comparison of the $N_{\rm coll}$ values obtained for the various estimators is reported in the table. The two different sets are consistent among each other and with the values calculated for Pb–p. The systematic uncertainties come from the uncertainty on the $N_{\rm coll}$ for 0–100% summed with the maximum difference between the $\langle N_{\rm coll}^{\rm mult}\rangle$ and $\langle N_{\rm coll}^{\rm Pb-side}\rangle$.

Figure 7 shows the distribution of the energy deposited in the Pb-going side (ZNA) calorimeter.

Table 5 reports the mean values of $\langle N_{\rm coll}^{\rm mult}\rangle$ and $\langle N_{\rm coll}^{\rm Pb-side}\rangle$, the maximum difference among the two, and the total systematic uncertainty.

The $T_{\rm pPb}$ values in Tab. 6 are calculated by dividing the $N_{\rm coll}$ values by the cross-section $\sigma_{\rm NN}^{\rm inel}$. The uncertainty is given by the quadrature sum of the maximum difference among the values calculated with

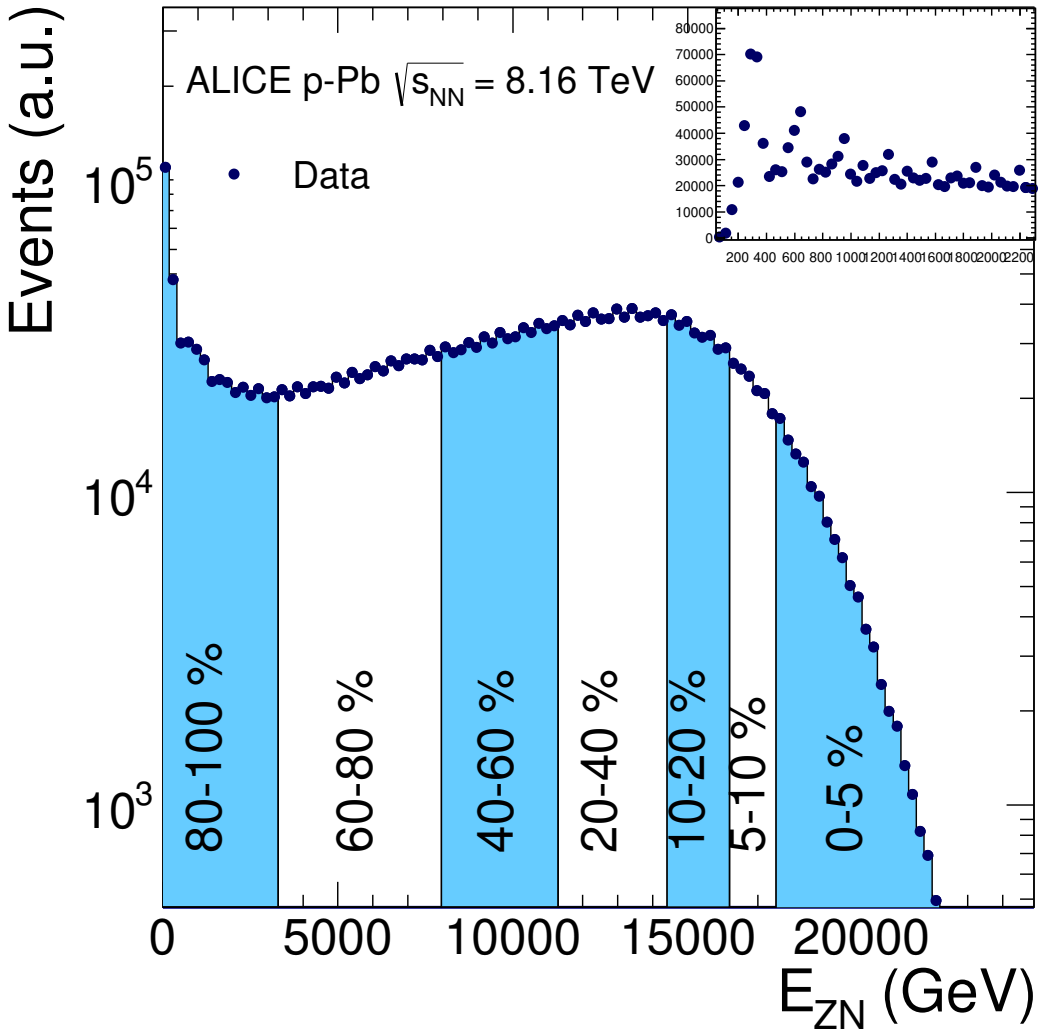

Fig. 7: Distribution of the energy deposited in the ZNA calorimeter.

different assumptions on the particle production mechanism, plus the uncerainty on the $T_{\rm pPb}$ for 0–100%.

Table 4: Geometric properties ($N_{\rm part}$, $N_{\rm coll}$, $T_{\rm pPb}$) of p–Pb collisions at $\sqrt{s_{\rm NN}}$ = 8.16 TeV. The mean values, the RMS, and the systematic uncertainties are obtained with a Glauber Monte Carlo calculation.

Centrality	$\langle N_{\rm part}\rangle$	RMS	(*sys.*)	$\langle N_{\rm coll}\rangle$	RMS	(*sys.*)	$\langle T_{\rm pPb}\rangle$ (1/mbarn)	RMS (1/mbarn)	(*sys.*) (1/mbarn)
0–100%	8.118	4.8	0.12	7.118	4.8	0.12	0.09818	0.071	0.002
V0A									
0–5%	16.21	3.86	0.208	15.21	3.86	0.208	0.2098	0.0532	0.00243
5–10%	14.43	3.78	0.172	13.43	3.78	0.172	0.1853	0.0521	0.00198
10–20%	12.98	3.85	0.159	11.98	3.85	0.159	0.1653	0.0531	0.002
20–40%	10.67	3.93	0.16	9.675	3.93	0.16	0.1334	0.0541	0.00218
40–60%	7.673	3.64	0.162	6.673	3.64	0.162	0.09204	0.0503	0.00226
60–80%	4.908	2.74	0.0902	3.908	2.74	0.0902	0.0539	0.0378	0.00116
80–100%	2.935	1.41	0.0431	1.935	1.41	0.0431	0.02669	0.0195	0.000548
0–20%	14.16	4.05	0.151	13.16	4.05	0.151	0.1814	0.0559	0.00177
60–100%	3.927	2.39	0.0523	2.927	2.39	0.0523	0.04037	0.033	0.000694
0–10%	15.32	3.92	0.179	14.32	3.92	0.179	0.1975	0.0541	0.002
10–20%	12.98	3.85	0.159	11.98	3.85	0.159	0.1653	0.0531	0.002
20–30%	11.42	3.87	0.164	10.42	3.87	0.164	0.1437	0.0534	0.0021
30–40%	9.941	3.84	0.147	8.941	3.84	0.147	0.1233	0.053	0.00198
40–50%	8.426	3.71	0.153	7.426	3.71	0.153	0.1024	0.0512	0.00216
50–60%	6.911	3.41	0.153	5.911	3.41	0.153	0.08153	0.0471	0.00211
60–70%	5.49	2.95	0.115	4.49	2.95	0.115	0.06194	0.0407	0.00155
70–80%	4.279	2.33	0.0672	3.279	2.33	0.0672	0.04522	0.0322	0.000843
80–90%	3.288	1.64	0.0412	2.288	1.64	0.0412	0.03155	0.0226	0.00049
90–100%	2.517	0.93	0.0195	1.517	0.93	0.0195	0.02093	0.0128	0.000278
V0M									
0–5%	17.49	3.32	0.226	16.49	3.32	0.226	0.2275	0.0458	0.00271
5–10%	15.31	3.03	0.152	14.31	3.03	0.152	0.1974	0.0418	0.00173
10–20%	13.61	3.02	0.164	12.61	3.02	0.164	0.1739	0.0417	0.00199
20–40%	10.96	3.07	0.136	9.957	3.07	0.136	0.1373	0.0424	0.00183
40–60%	7.465	2.84	0.0833	6.465	2.84	0.0833	0.08917	0.0392	0.00128
60–80%	4.354	2.04	0.0683	3.354	2.04	0.0683	0.04626	0.0282	0.000952
80–100%	2.619	0.986	0.0153	1.619	0.986	0.0153	0.02233	0.0136	0.000239
0–20%	15.01	3.49	0.161	14.01	3.49	0.161	0.1932	0.0481	0.00187
60–100%	3.481	1.82	0.0396	2.481	1.82	0.0396	0.03422	0.0251	0.000535
0–10%	16.41	3.36	0.186	15.41	3.36	0.186	0.2126	0.0464	0.00217
10–20%	13.61	3.02	0.164	12.61	3.02	0.164	0.1739	0.0417	0.00199
20–30%	11.8	2.98	0.15	10.8	2.98	0.15	0.149	0.0411	0.00196
30–40%	10.11	2.93	0.119	9.106	2.93	0.119	0.1256	0.0404	0.00169
40–50%	8.338	2.82	0.116	7.338	2.82	0.116	0.1012	0.0389	0.00175
50–60%	6.588	2.58	0.102	5.588	2.58	0.102	0.07707	0.0356	0.00155
60–70%	4.971	2.19	0.0965	3.971	2.19	0.0965	0.05478	0.0302	0.00134
70–80%	3.73	1.67	0.0417	2.73	1.67	0.0417	0.03766	0.023	0.00059
80–90%	2.898	1.15	0.029	1.898	1.15	0.029	0.02618	0.0159	0.000442
90–100%	2.324	0.654	0.0193	1.324	0.654	0.0193	0.01827	0.00903	0.000285
CL1									
0–5%	17	3.54	0.353	16	3.54	0.353	0.2207	0.0489	0.00471
5–10%	15.01	3.32	0.282	14.01	3.32	0.282	0.1932	0.0459	0.00371
10–20%	13.38	3.36	0.187	12.38	3.36	0.187	0.1708	0.0463	0.00209
20–40%	10.81	3.44	0.166	9.813	3.44	0.166	0.1353	0.0475	0.00211
40–60%	7.475	3.18	0.191	6.475	3.18	0.191	0.08931	0.0439	0.00259
60–80%	4.495	2.31	0.143	3.495	2.31	0.143	0.04821	0.0319	0.00197
80–100%	2.709	1.12	0.113	1.709	1.12	0.113	0.02358	0.0154	0.00158
0–20%	14.7	3.71	0.24	13.7	3.71	0.24	0.1889	0.0511	0.0029
60–100%	3.636	2.04	0.0784	2.636	2.04	0.0784	0.03636	0.0281	0.00103
0–10%	16.02	3.58	0.349	15.02	3.58	0.349	0.2072	0.0493	0.00457
10–20%	13.38	3.36	0.187	12.38	3.36	0.187	0.1708	0.0463	0.00209
20–30%	11.66	3.35	0.101	10.66	3.35	0.101	0.147	0.0462	0.000995
30–40%	9.982	3.33	0.159	8.982	3.33	0.159	0.1239	0.0459	0.00229
40–50%	8.301	3.22	0.195	7.301	3.22	0.195	0.1007	0.0444	0.00263
50–60%	6.693	2.95	0.177	5.693	2.95	0.177	0.07853	0.0408	0.00233
60–70%	5.153	2.52	0.113	4.153	2.52	0.113	0.05728	0.0347	0.00147
70–80%	3.887	1.92	0.152	2.887	1.92	0.152	0.03981	0.0264	0.00209
80–90%	2.995	1.31	0.189	1.995	1.31	0.189	0.02752	0.018	0.00263
90–100%	2.388	0.749	0.104	1.388	0.749	0.104	0.01914	0.0103	0.00145

Table 5: $\langle N_{\rm coll} \rangle$ values of p–Pb collisions at $\sqrt{s_{\rm NN}}$ = 8.16 TeV obtained with the hybrid method.

Centrality	$N_{\rm coll}^{\rm mult}$	$N_{\rm coll}^{\rm Pb-side}$	max diff (%)	tot sys (%)
0–5%	13.4	14.2	6.0	6.2
5–10%	12.5	12.9	3.2	3.6
10–20%	11.5	11.8	2.5	3.1
20–40%	9.81	9.77	0.4	1.7
40–60%	7.09	6.83	3.7	4.1
60–80%	4.28	4.09	4.3	4.6
80–100%	2.05	2.10	2.4	2.9
0–10%	12.9	13.6	5.4	5.7
10–20%	11.5	11.8	2.5	3.0
20–30%	10.4	10.5	1.0	1.8
30–40%	9.21	9.09	1.3	2.0
40–50%	7.82	7.58	3.1	3.4
50–60%	6.37	6.09	4.4	4.6
60–70%	4.93	4.69	4.9	5.1
70–80%	3.63	3.48	4.1	4.4
80–90%	2.53	2.51	0.8	1.7
90–100%	1.58	1.70	7.6	7.7
0–2%	13.9	14.7	5.4	5.6
2–10%	12.7	13.3	4.5	4.8
0–20%	12.2	12.7	3.9	4.3
60-100%	3.17	3.10	2.2	2.8
80–90%	2.53	2.51	0.8	1.9
0–90%	7.71	7.70	0.1	1.7

Table 6: $\langle T_{\rm pPb} \rangle$ values of p–Pb collisions at $\sqrt{s_{\rm NN}}$ = 8.16 TeV obtained with the hybrid method.

Centrality	$T_{\rm pPb}^{\rm mult}$	$T_{\rm pPb}^{\rm Pb-side}$	max diff (%)	tot sys (%)
0–5%	0.185	0.195	6.0	6.4
5–10%	0.172	0.178	3.2	3.8
10–20%	0.159	0.163	2.5	3.3
20–40%	0.135	0.135	0.4	2.1
40–60%	0.0978	0.0942	3.7	4.2
60–80%	0.0590	0.0564	4.3	4.8
80–100%	0.0287	0.0294	2.4	3.1
0–10%	0.178	0.188	5.4	5.8
10–20%	0.159	0.163	2.5	3.2
20–30%	0.143	0.145	1.0	2.2
30–40%	0.127	0.125	1.3	2.4
40–50%	0.108	0.105	3.1	3.7
50–60%	0.0879	0.0834	4.4	4.8
60–70%	0.0680	0.0647	4.9	5.3
70–80%	0.0501	0.0480	4.1	4.6
80–90%	0.0349	0.0346	0.8	2.1
90–100%	0.0218	0.0234	7.6	7.8
0–2%	0.192	0.203	5.4	5.6
2–10%	0.175	0.183	4.5	4.8
0–20%	0.168	0.175	3.9	4.4
60-100%	0.0437	0.0427	2.2	3.0
80–90%	0.0349	0.0346	0.8	1.9
0–90%	0.106	0.106	0.1	1.7

7 p-Pb collisions at $\sqrt{s_{\rm NN}}$ = 5.02 TeV

Table 7 shows the geometric properties ($N_{\rm part}$, $N_{\rm coll}$, $T_{\rm pPb}$) of p–Pb collisions at $\sqrt{s_{\rm NN}}$ = 5.02 TeV for centrality classes defined by sharp cuts in the V0A, V0M or CL1 multiplicity distribution.

For the calculations with the hybrid method we use another assumption on particle production, namely that the yield of charged high-$p_{\rm t}$particles at mid-rapidity is proportional to the number of binary NN collisions ($N_{\rm coll}$), in order to calculate the set of $N_{\rm coll}^{\rm high-p_t}$, restricted however only to the classes with the $p_{\rm t}$-spectra were calculated, or those which can be derived with weigthed average.

Table 7: Geometric properties ($N_{\rm part}$, $N_{\rm coll}$, $T_{\rm pPb}$) of p–Pb collisions at $\sqrt{s_{\rm NN}}$ = 5.02 TeV. The mean values, the RMS, and the systematic uncertainties are obtained with a Glauber Monte Carlo calculation.

Centrality	$\langle N_{\rm part}\rangle$	RMS	(*sys.*)	$\langle N_{\rm coll}\rangle$	RMS	(*sys.*)	$\langle T_{\rm pPb}\rangle$ (1/mbarn)	RMS (1/mbarn)	(*sys.*) (1/mbarn)
0–100%	7.708	4.8	0.11	6.708	4.8	0.11	0.09923	0.071	0.0017
V0A									
0–5%	15.1	3.77	0.747	14.1	3.77	0.747	0.2085	0.0557	0.00997
5–10%	13.47	3.7	0.687	12.47	3.7	0.687	0.1845	0.0547	0.00919
10–20%	12.18	3.78	0.612	11.18	3.78	0.612	0.1654	0.0559	0.00813
20–40%	10.09	3.84	0.472	9.089	3.84	0.472	0.1345	0.0568	0.00624
40–60%	7.42	3.57	0.272	6.42	3.57	0.272	0.09496	0.0529	0.00357
60–80%	4.884	2.73	0.0974	3.884	2.73	0.0974	0.05745	0.0404	0.00127
80–100%	2.982	1.47	0.0331	1.982	1.47	0.0331	0.02932	0.0217	0.000468
0–20%	13.23	3.94	0.673	12.23	3.94	0.673	0.181	0.0583	0.00898
60–100%	3.93	2.38	0.1	2.93	2.38	0.1	0.04334	0.0353	0.00138
0–10%	14.29	3.82	0.712	13.29	3.82	0.712	0.1966	0.0565	0.0095
10–20%	12.18	3.78	0.612	11.18	3.78	0.612	0.1654	0.0559	0.00813
20–30%	10.76	3.8	0.542	9.759	3.8	0.542	0.1444	0.0562	0.00715
30–40%	9.451	3.77	0.391	8.451	3.77	0.391	0.125	0.0557	0.00508
40–50%	8.075	3.64	0.333	7.075	3.64	0.333	0.1047	0.0538	0.00441
50–60%	6.755	3.38	0.222	5.755	3.38	0.222	0.08513	0.05	0.0029
60–70%	5.437	2.93	0.186	4.437	2.93	0.186	0.06564	0.0434	0.00258
70–80%	4.306	2.37	0.0731	3.306	2.37	0.0731	0.04891	0.035	0.00105
80–90%	3.365	1.72	0.0628	2.365	1.72	0.0628	0.03499	0.0254	0.000889
90–100%	2.571	0.995	0.0287	1.571	0.995	0.0287	0.02324	0.0147	0.00038
V0M									
0–5%	16.51	3.2	0.804	15.51	3.2	0.804	0.2294	0.0473	0.0107
5–10%	14.44	2.94	0.695	13.44	2.94	0.695	0.1989	0.0435	0.00922
10–20%	12.87	2.91	0.626	11.87	2.91	0.626	0.1757	0.043	0.00825
20–40%	10.4	2.95	0.474	9.396	2.95	0.474	0.139	0.0437	0.00623
40–60%	7.169	2.76	0.251	6.169	2.76	0.251	0.09125	0.0408	0.00327
60–80%	4.253	1.98	0.112	3.253	1.98	0.112	0.04812	0.0294	0.00151
80–100%	2.6	0.968	0.0373	1.6	0.968	0.0373	0.02367	0.0143	0.000552
0–20%	14.18	3.34	0.69	13.18	3.34	0.69	0.1949	0.0494	0.00913
60–100%	3.434	1.77	0.0639	2.434	1.77	0.0639	0.03601	0.0262	0.00082
0–10%	15.47	3.24	0.749	14.47	3.24	0.749	0.2141	0.0479	0.00997
10–20%	12.87	2.91	0.626	11.87	2.91	0.626	0.1757	0.043	0.00825
20–30%	11.18	2.87	0.546	10.18	2.87	0.546	0.1506	0.0425	0.00723
30–40%	9.613	2.83	0.417	8.613	2.83	0.417	0.1274	0.0418	0.00545
40–50%	7.994	2.74	0.288	6.994	2.74	0.288	0.1035	0.0406	0.00373
50–60%	6.325	2.51	0.214	5.325	2.51	0.214	0.07878	0.0372	0.00284
60–70%	4.85	2.13	0.137	3.85	2.13	0.137	0.05696	0.0316	0.00177
70–80%	3.682	1.64	0.0682	2.682	1.64	0.0682	0.03968	0.0243	0.000846
80–90%	2.876	1.14	0.0607	1.876	1.14	0.0607	0.02775	0.0168	0.000879
90–100%	2.323	0.653	0.0248	1.323	0.653	0.0248	0.01957	0.00966	0.000344
CL1									
0–5%	15.97	3.41	0.856	14.97	3.41	0.856	0.2214	0.0505	0.0118
5–10%	14.05	3.25	0.743	13.05	3.25	0.743	0.193	0.048	0.0102
10–20%	12.62	3.27	0.607	11.62	3.27	0.607	0.1719	0.0483	0.00815
20–40%	10.31	3.33	0.458	9.312	3.33	0.458	0.1377	0.0492	0.00599
40–60%	7.273	3.13	0.28	6.273	3.13	0.28	0.0928	0.0462	0.0037
60–80%	4.485	2.29	0.187	3.485	2.29	0.187	0.05156	0.0339	0.00255
80–100%	2.744	1.16	0.0863	1.744	1.16	0.0863	0.02579	0.0172	0.00116
0–20%	13.85	3.57	0.678	12.85	3.57	0.678	0.1901	0.0528	0.00913
60–100%	3.624	2.01	0.128	2.624	2.01	0.128	0.03881	0.0298	0.00181
0–10%	15.01	3.46	0.773	14.01	3.46	0.773	0.2073	0.0512	0.0106
10–20%	12.62	3.27	0.607	11.62	3.27	0.607	0.1719	0.0483	0.00815
20–30%	11.03	3.26	0.529	10.03	3.26	0.529	0.1483	0.0483	0.00707
30–40%	9.54	3.23	0.42	8.54	3.23	0.42	0.1263	0.0478	0.00551
40–50%	7.998	3.16	0.324	6.998	3.16	0.324	0.1035	0.0467	0.00426
50–60%	6.476	2.89	0.241	5.476	2.89	0.241	0.081	0.0428	0.00329
60–70%	5.077	2.47	0.249	4.077	2.47	0.249	0.06031	0.0366	0.00353
70–80%	3.914	1.94	0.208	2.914	1.94	0.208	0.04311	0.0287	0.00291
80–90%	3.077	1.38	0.157	2.077	1.38	0.157	0.03073	0.0204	0.00224
90–100%	2.441	0.821	0.105	1.441	0.821	0.105	0.02132	0.0121	0.00154

Table 8: $\langle N_{\mathrm{coll}} \rangle$ values of p–Pb collisions at $\sqrt{s_{\mathrm{NN}}}$ = 5.02 TeV obtained with the hybrid method.

Centrality	$N_{\mathrm{coll}}^{\mathrm{mult}}$	$N_{\mathrm{coll}}^{\mathrm{high-p_t}}$	$N_{\mathrm{coll}}^{\mathrm{Pb-side}}$	max diff (%)	tot sys (%)
0–5%	11.9	12.2	12.9	8.4	8.6
5–10%	11.3	11.8	11.9	5.3	5.5
10–20%	10.7	11.0	11.1	3.7	4.1
20–40%	9.29	9.45	9.32	1.7	2.4
40–60%	6.87	6.62	6.54	4.8	5.1
60–80%	4.17	3.93	3.89	6.9	7.1
80–100%	2.03	1.97	2.00	2.9	3.3
0–10%	11.6	12.0	12.4	6.9	7.1
10–20%	10.7	11.0	11.1	3.7	4.1
20–30%	9.82	-	9.94	1.2	2.0
30–40%	8.76	-	8.69	0.8	1.8
40–50%	7.57	-	7.29	3.7	4.0
50–60%	6.17	-	5.80	6.0	6.2
60–70%	4.80	-	4.45	7.3	7.5
70–80%	3.55	-	3.30	7.0	7.2
80–90%	2.39	-	2.37	0.8	1.8
90–100%	1.58	-	1.63	3.2	3.6
0–2%	12.4	-	13.2	6.4	6.6
2–10%	11.4	-	12.2	7.0	7.2
0–20%	11.1	11.5	11.7	5.4	5.6
60-100%	3.10	2.95	2.94	5.2	5.4
80–90%	2.09	-	1.98	5.3	5.5
0–90%	6.50	-	6.50	0.0	1.6

Table 9: $\langle T_{\mathrm{pPb}} \rangle$ values of p–Pb collisions at $\sqrt{s_{\mathrm{NN}}}$ = 5.02 TeV obtained with the hybrid method.

Centrality	$T_{\mathrm{pPb}}^{\mathrm{mult}}$	$T_{\mathrm{pPb}}^{\mathrm{high-p_t}}$	$T_{\mathrm{pPb}}^{\mathrm{Pb-side}}$	max diff (%)	tot sys (%)
0–5%	0.176	0.180	0.191	8.4	8.6
5–10%	0.167	0.174	0.176	5.3	5.6
10–20%	0.158	0.163	0.164	3.7	4.1
20–40%	0.137	0.140	0.138	1.7	2.4
40–60%	0.102	0.0979	0.0967	4.8	5.1
60–80%	0.0617	0.0581	0.0575	6.9	7.1
80–100%	0.0300	0.0291	0.0296	2.9	3.4
0–10%	0.172	0.178	0.183	6.9	7.1
10–20%	0.158	0.163	0.164	3.7	4.1
20–30%	0.145	-	0.147	1.2	2.1
30–40%	0.130	-	0.129	0.8	1.9
40–50%	0.112	-	0.108	3.7	4.1
50–60%	0.0913	-	0.0858	6.0	6.2
60–70%	0.0710	-	0.0658	7.3	7.5
70–80%	0.0525	-	0.0488	7.0	7.2
80–90%	0.0353	-	0.0351	0.8	1.9
90–100%	0.0234	-	0.0241	3.2	3.6
0–2%	0.183	-	0.195	6.4	6.6
2–10%	0.169	-	0.180	7.0	7.2
0–20%	0.164	0.170	0.173	5.4	5.7
60-100%	0.0459	0.0436	0.0435	5.2	5.4
80–90%	0.0309	-	0.0293	5.3	5.5
0–90%	0.0961	-	0.0961	0.0	1.6

Acknowledgements

The ALICE Collaboration would like to thank all its engineers and technicians for their invaluable contributions to the construction of the experiment and the CERN accelerator teams for the outstanding performance of the LHC complex. The ALICE Collaboration gratefully acknowledges the resources and support provided by all Grid centres and the Worldwide LHC Computing Grid (WLCG) collaboration. The ALICE Collaboration acknowledges the following funding agencies for their support in building and running the ALICE detector: A. I. Alikhanyan National Science Laboratory (Yerevan Physics Institute) Foundation (ANSL), State Committee of Science and World Federation of Scientists (WFS), Armenia; Austrian Academy of Sciences, Austrian Science Fund (FWF): [M 2467-N36] and Nationalstiftung für Forschung, Technologie und Entwicklung, Austria; Ministry of Communications and High Technologies, National Nuclear Research Center, Azerbaijan; Conselho Nacional de Desenvolvimento Científico e Tecnológico (CNPq), Financiadora de Estudos e Projetos (Finep), Fundação de Amparo à Pesquisa do Estado de São Paulo (FAPESP) and Universidade Federal do Rio Grande do Sul (UFRGS), Brazil; Ministry of Education of China (MOEC) , Ministry of Science & Technology of China (MSTC) and National Natural Science Foundation of China (NSFC), China; Ministry of Science and Education and Croatian Science Foundation, Croatia; Centro de Aplicaciones Tecnológicas y Desarrollo Nuclear (CEADEN), Cubaenergía, Cuba; Ministry of Education, Youth and Sports of the Czech Republic, Czech Republic; The Danish Council for Independent Research | Natural Sciences, the VILLUM FONDEN and Danish National Research Foundation (DNRF), Denmark; Helsinki Institute of Physics (HIP), Finland; Commissariat à l'Energie Atomique (CEA) and Institut National de Physique Nucléaire et de Physique des Particules (IN2P3) and Centre National de la Recherche Scientifique (CNRS), France; Bundesministerium für Bildung und Forschung (BMBF) and GSI Helmholtzzentrum für Schwerionenforschung GmbH, Germany; General Secretariat for Research and Technology, Ministry of Education, Research and Religions, Greece; National Research, Development and Innovation Office, Hungary; Department of Atomic Energy Government of India (DAE), Department of Science and Technology, Government of India (DST), University Grants Commission, Government of India (UGC) and Council of Scientific and Industrial Research (CSIR), India; Indonesian Institute of Science, Indonesia; Istituto Nazionale di Fisica Nucleare (INFN), Italy; Institute for Innovative Science and Technology , Nagasaki Institute of Applied Science (IIST), Japanese Ministry of Education, Culture, Sports, Science and Technology (MEXT) and Japan Society for the Promotion of Science (JSPS) KAKENHI, Japan; Consejo Nacional de Ciencia (CONACYT) y Tecnología, through Fondo de Cooperación Internacional en Ciencia y Tecnología (FONCICYT) and Dirección General de Asuntos del Personal Academico (DGAPA), Mexico; Nederlandse Organisatie voor Wetenschappelijk Onderzoek (NWO), Netherlands; The Research Council of Norway, Norway; Commission on Science and Technology for Sustainable Development in the South (COMSATS), Pakistan; Pontificia Universidad Católica del Perú, Peru; Ministry of Science and Higher Education, National Science Centre and WUT ID-UB, Poland; Korea Institute of Science and Technology Information and National Research Foundation of Korea (NRF), Republic of Korea; Ministry of Education and Scientific Research, Institute of Atomic Physics and Ministry of Research and Innovation and Institute of Atomic Physics, Romania; Joint Institute for Nuclear Research (JINR), Ministry of Education and Science of the Russian Federation, National Research Centre Kurchatov Institute, Russian Science Foundation and Russian Foundation for Basic Research, Russia; Ministry of Education, Science, Research and Sport of the Slovak Republic, Slovakia; National Research Foundation of South Africa, South Africa; Swedish Research Council (VR) and Knut & Alice Wallenberg Foundation (KAW), Sweden; European Organization for Nuclear Research, Switzerland; Suranaree University of Technology (SUT), National Science and Technology Development Agency (NSDTA) and Office of the Higher Education Commission under NRU project of Thailand, Thailand; Turkish Atomic Energy Agency (TAEK), Turkey; National Academy of Sciences of Ukraine, Ukraine; Science and Technology Facilities Council (STFC), United Kingdom; National Science Foundation of

the United States of America (NSF) and United States Department of Energy, Office of Nuclear Physics (DOE NP), United States of America.

References

[1] **ALICE** Collaboration, B. Abelev *et al.*, "Centrality determination of Pb-Pb collisions at $\sqrt{s_{\rm NN}}$ = 2.76 TeV with ALICE," *Phys.Rev.* **C88** no. 4, (2013) 044909, arXiv:1301.4361 [nucl-ex].

[2] **ALICE** Collaboration, J. Adam *et al.*, "Centrality dependence of particle production in p-Pb collisions at $\sqrt{s_{\rm NN}}$= 5.02 TeV," *Phys. Rev.* **C91** no. 6, (2015) 064905, arXiv:1412.6828 [nucl-ex].

[3] M. Miller, K. Reygers, S. J. Sanders, and P. Steinberg, "Glauber modeling in high energy nuclear collisions," *Ann. Rev. Nucl. Part. Sci.* **57** (2007) 205–243, arXiv:nucl-ex/0701025.

[4] R. Glauber, "Cross sections in deuterium at high energies," *Phys. Rev.* **100** (1955) 242.

[5] R. Glauber, "Lectures in theoretical physics," *ed WE Brittin and LG Dunham* **1** (1959) 315.

[6] R. Glauber, "Quantum optics and heavy ion physics," *Nucl. Phys.* **A 774** (2006) 3.

[7] A. P. T.W. Ludlam and A. Shor, "Hijet. a monte carlo event generator for p–nucleus and nucleus–nucleus collisions," *BNL* **37196** (1985) 373–381.

[8] A. Shor and R. Longacre, "Effects of secondary interactions in proton-nucleus and nucleus-nucleus collisions using the hijet event generator," *Phys. Lett.* **B 218** (1989) 100.

[9] B. Alver, M. Baker, C. Loizides, and P. Steinberg, "The PHOBOS Glauber Monte Carlo," arXiv:0805.4411 [nucl-ex].

[10] H. De Vries, C. W. De Jager, and C. De Vries, "Nuclear charge and magnetization density distribution parameters from elastic electron scattering," *Atom. Data Nucl. Data Tabl.* **36** (1987) 495–536.

[11] C. Loizides, J. Kamin, and D. d'Enterria, "Precision Monte Carlo Glauber predictions at present and future nuclear colliders," arXiv:1710.07098 [nucl-ex].

[12] **ALICE** Collaboration, K. Aamodt *et al.*, "First proton-proton collisions at the LHC as observed with the ALICE detector: Measurement of the charged particle pseudorapidity density at s**(1/2) = 900-GeV," *Eur. Phys. J. C* **65** (2010) 111–125, arXiv:0911.5430 [hep-ex].

[13] **ALICE** Collaboration, K. Aamodt *et al.*, "Charged-particle multiplicity measurement in proton-proton collisions at $\sqrt{s}$ = 0.9 and 2.36 TeV with ALICE at LHC," *Eur. Phys. J. C* **68** (2010) 89–108, arXiv:1004.3034 [hep-ex].

[14] D. Kharzeev, E. Levin, and M. Nardi, "Color glass condensate at the LHC: Hadron multiplicities in p p, p A and A A collisions," *Nucl. Phys.* **A747** (2005) 609–629, arXiv:hep-ph/0408050.

[15] W. Deng, X. Wang, and R. Xu, "Hadron production in $p+p$, $p+Pb$ and $Pb+Pb$ collisions at the LHC energies with HIJING2.0 model," arXiv:1008.1841 [hep-ph].

A The ALICE Collaboration

ALICE Collaboration

S. Acharya[142], D. Adamová[97], A. Adler[75], J. Adolfsson[82], G. Aglieri Rinella[35], M. Agnello[31], N. Agrawal[55], Z. Ahammed[142], S. Ahmad[16], S.U. Ahn[77], Z. Akbar[52], A. Akindinov[94], M. Al-Turany[109], D.S.D. Albuquerque[124], D. Aleksandrov[90], B. Alessandro[60], H.M. Alfanda[7], R. Alfaro Molina[72], B. Ali[16], Y. Ali[14], A. Alici[26], N. Alizadehvandchali[127], A. Alkin[35], J. Alme[21], T. Alt[69], L. Altenkamper[21], I. Altsybeev[115], M.N. Anaam[7], C. Andrei[49], D. Andreou[92], A. Andronic[145], M. Angeletti[35], V. Anguelov[106], T. Antičić[110], F. Antinori[58], P. Antonioli[55], N. Apadula[81], L. Aphecetche[117], H. Appelshäuser[69], S. Arcelli[26], R. Arnaldi[60], M. Arratia[81], I.C. Arsene[20], M. Arslandok[147,106], A. Augustinus[35], R. Averbeck[109], S. Aziz[79], M.D. Azmi[16], A. Badalà[57], Y.W. Baek[42], X. Bai[109], R. Bailhache[69], R. Bala[103], A. Balbino[31], A. Baldisseri[139], M. Ball[44], D. Banerjee[4], R. Barbera[27], L. Barioglio[25], M. Barlou[86], G.G. Barnaföldi[146], L.S. Barnby[96], V. Barret[136], C. Bartels[129], K. Barth[35], E. Bartsch[69], F. Baruffaldi[28], N. Bastid[136], S. Basu[82,144], G. Batigne[117], B. Batyunya[76], D. Bauri[50], J.L. Bazo Alba[114], I.G. Bearden[91], C. Beattie[147], I. Belikov[138], A.D.C. Bell Hechavarria[145], F. Bellini[35], R. Bellwied[127], S. Belokurova[115], V. Belyaev[95], G. Bencedi[70,146], S. Beole[25], A. Bercuci[49], Y. Berdnikov[100], A. Berdnikova[106], D. Berenyi[146], L. Bergmann[106], M.G. Besoiu[68], L. Betev[35], P.P. Bhaduri[142], A. Bhasin[103], I.R. Bhat[103], M.A. Bhat[4], B. Bhattacharjee[43], P. Bhattacharya[23], A. Bianchi[25], L. Bianchi[25], N. Bianchi[53], J. Bielčík[38], J. Bielčíková[97], A. Bilandzic[107], G. Biro[146], S. Biswas[4], J.T. Blair[121], D. Blau[90], M.B. Blidaru[109], C. Blume[69], G. Boca[29], F. Bock[98], A. Bogdanov[95], S. Boi[23], J. Bok[62], L. Boldizsár[146], A. Bolozdynya[95], M. Bombara[39], G. Bonomi[141], H. Borel[139], A. Borissov[83,95], H. Bossi[147], E. Botta[25], L. Bratrud[69], P. Braun-Munzinger[109], M. Bregant[123], M. Broz[38], G.E. Bruno[108,34], M.D. Buckland[129], D. Budnikov[111], H. Buesching[69], S. Bufalino[31], O. Bugnon[117], P. Buhler[116], P. Buncic[35], Z. Buthelezi[73,133], J.B. Butt[14], S.A. Bysiak[120], D. Caffarri[92], A. Caliva[109], E. Calvo Villar[114], J.M.M. Camacho[122], R.S. Camacho[46], P. Camerini[24], F.D.M. Canedo[123], A.A. Capon[116], F. Carnesecchi[26], R. Caron[139], J. Castillo Castellanos[139], E.A.R. Casula[56], F. Catalano[31], C. Ceballos Sanchez[76], P. Chakraborty[50], S. Chandra[142], W. Chang[7], S. Chapeland[35], M. Chartier[129], S. Chattopadhyay[142], S. Chattopadhyay[112], A. Chauvin[23], C. Cheshkov[137], B. Cheynis[137], V. Chibante Barroso[35], D.D. Chinellato[124], S. Cho[62], P. Chochula[35], P. Christakoglou[92], C.H. Christensen[91], P. Christiansen[82], T. Chujo[135], C. Cicalo[56], L. Cifarelli[26], F. Cindolo[55], M.R. Ciupek[109], G. Clai[II,55], J. Cleymans[126], F. Colamaria[54], J.S. Colburn[113], D. Colella[54], A. Collu[81], M. Colocci[35,26], M. Concas[III,60], G. Conesa Balbastre[80], Z. Conesa del Valle[79], G. Contin[24], J.G. Contreras[38], T.M. Cormier[98], P. Cortese[32], M.R. Cosentino[125], F. Costa[35], S. Costanza[29], P. Crochet[136], E. Cuautle[70], P. Cui[7], L. Cunqueiro[98], T. Dahms[107], A. Dainese[58], F.P.A. Damas[117,139], M.C. Danisch[106], A. Danu[68], D. Das[112], I. Das[112], P. Das[88], P. Das[4], S. Das[4], S. Dash[50], S. De[88], A. De Caro[30], G. de Cataldo[54], L. De Cilladi[25], J. de Cuveland[40], A. De Falco[23], D. De Gruttola[30], N. De Marco[60], C. De Martin[24], S. De Pasquale[30], S. Deb[51], H.F. Degenhardt[123], K.R. Deja[143], S. Delsanto[25], W. Deng[7], P. Dhankher[50], D. Di Bari[34], A. Di Mauro[35], R.A. Diaz[8], T. Dietel[126], P. Dillenseger[69], Y. Ding[7], R. Divià[35], D.U. Dixit[19], Ø. Djuvsland[21], U. Dmitrieva[64], J. Do[62], A. Dobrin[68], B. Dönigus[69], O. Dordic[20], A.K. Dubey[142], A. Dubla[109,92], S. Dudi[102], M. Dukhishyam[88], P. Dupieux[136], T.M. Eder[145], R.J. Ehlers[98], V.N. Eikeland[21], D. Elia[54], B. Erazmus[117], F. Erhardt[101], A. Erokhin[115], M.R. Ersdal[21], B. Espagnon[79], G. Eulisse[35], D. Evans[113], S. Evdokimov[93], L. Fabbietti[107], M. Faggin[28], J. Faivre[80], F. Fan[7], A. Fantoni[53], M. Fasel[98], P. Fecchio[31], A. Feliciello[60], G. Feofilov[115], A. Fernández Téllez[46], A. Ferrero[139], A. Ferretti[25], A. Festanti[35], V.J.G. Feuillard[106], J. Figiel[120], S. Filchagin[111], D. Finogeev[64], F.M. Fionda[21], G. Fiorenza[54], F. Flor[127], A.N. Flores[121], S. Foertsch[73], P. Foka[109], S. Fokin[90], E. Fragiacomo[61], U. Fuchs[35], C. Furget[80], A. Furs[64], M. Fusco Girard[30], J.J. Gaardhøje[91], M. Gagliardi[25], A.M. Gago[114], A. Gal[138], C.D. Galvan[122], P. Ganoti[86], C. Garabatos[109], J.R.A. Garcia[46], E. Garcia-Solis[10], K. Garg[117], C. Gargiulo[35], A. Garibli[89], K. Garner[145], P. Gasik[107],

E.F. Gauger[121], M.B. Gay Ducati[71], M. Germain[117], J. Ghosh[112], P. Ghosh[142], S.K. Ghosh[4], M. Giacalone[26], P. Gianotti[53], P. Giubellino[109,60], P. Giubilato[28], A.M.C. Glaenzer[139], P. Glässel[106], V. Gonzalez[144], L.H. González-Trueba[72], S. Gorbunov[40], L. Görlich[120], S. Gotovac[36], V. Grabski[72], L.K. Graczykowski[143], K.L. Graham[113], L. Greiner[81], A. Grelli[63], C. Grigoras[35], V. Grigoriev[95], A. Grigoryan[I,1], S. Grigoryan[76], O.S. Groettvik[21], F. Grosa[60], J.F. Grosse-Oetringhaus[35], R. Grosso[109], R. Guernane[80], M. Guilbaud[117], M. Guittiere[117], K. Gulbrandsen[91], T. Gunji[134], A. Gupta[103], R. Gupta[103], I.B. Guzman[46], R. Haake[147], M.K. Habib[109], C. Hadjidakis[79], H. Hamagaki[84], G. Hamar[146], M. Hamid[7], R. Hannigan[121], M.R. Haque[143,88], A. Harlenderova[109], J.W. Harris[147], A. Harton[10], J.A. Hasenbichler[35], H. Hassan[98], D. Hatzifotiadou[55], P. Hauer[44], L.B. Havener[147], S. Hayashi[134], S.T. Heckel[107], E. Hellbär[69], H. Helstrup[37], T. Herman[38], E.G. Hernandez[46], G. Herrera Corral[9], F. Herrmann[145], K.F. Hetland[37], H. Hillemanns[35], C. Hills[129], B. Hippolyte[138], B. Hohlweger[107], J. Honermann[145], G.H. Hong[148], D. Horak[38], S. Hornung[109], R. Hosokawa[15], P. Hristov[35], C. Huang[79], C. Hughes[132], P. Huhn[69], T.J. Humanic[99], H. Hushnud[112], L.A. Husova[145], N. Hussain[43], D. Hutter[40], J.P. Iddon[35,129], R. Ilkaev[111], H. Ilyas[14], M. Inaba[135], G.M. Innocenti[35], M. Ippolitov[90], A. Isakov[38,97], M.S. Islam[112], M. Ivanov[109], V. Ivanov[100], V. Izucheev[93], B. Jacak[81], N. Jacazio[35,55], P.M. Jacobs[81], S. Jadlovska[119], J. Jadlovsky[119], S. Jaelani[63], C. Jahnke[123], M.J. Jakubowska[143], M.A. Janik[143], T. Janson[75], M. Jercic[101], O. Jevons[113], M. Jin[127], F. Jonas[98,145], P.G. Jones[113], J. Jung[69], M. Jung[69], A. Jusko[113], P. Kalinak[65], A. Kalweit[35], V. Kaplin[95], S. Kar[7], A. Karasu Uysal[78], D. Karatovic[101], O. Karavichev[64], T. Karavicheva[64], P. Karczmarczyk[143], E. Karpechev[64], A. Kazantsev[90], U. Kebschull[75], R. Keidel[48], M. Keil[35], B. Ketzer[44], Z. Khabanova[92], A.M. Khan[7], S. Khan[16], A. Khanzadeev[100], Y. Kharlov[93], A. Khatun[16], A. Khuntia[120], B. Kileng[37], B. Kim[62], D. Kim[148], D.J. Kim[128], E.J. Kim[74], H. Kim[17], J. Kim[148], J.S. Kim[42], J. Kim[106], J. Kim[148], J. Kim[74], M. Kim[106], S. Kim[18], T. Kim[148], T. Kim[148], S. Kirsch[69], I. Kisel[40], S. Kiselev[94], A. Kisiel[143], J.L. Klay[6], J. Klein[35,60], S. Klein[81], C. Klein-Bösing[145], M. Kleiner[69], T. Klemenz[107], A. Kluge[35], A.G. Knospe[127], C. Kobdaj[118], M.K. Köhler[106], T. Kollegger[109], A. Kondratyev[76], N. Kondratyeva[95], E. Kondratyuk[93], J. Konig[69], S.A. Konigstorfer[107], P.J. Konopka[2,35], G. Kornakov[143], S.D. Koryciak[2], L. Koska[119], O. Kovalenko[87], V. Kovalenko[115], M. Kowalski[120], I. Králik[65], A. Kravčáková[39], L. Kreis[109], M. Krivda[113,65], F. Krizek[97], K. Krizkova Gajdosova[38], M. Kroesen[106], M. Krüger[69], E. Kryshen[100], M. Krzewicki[40], V. Kučera[35], C. Kuhn[138], P.G. Kuijer[92], T. Kumaoka[135], L. Kumar[102], S. Kundu[88], P. Kurashvili[87], A. Kurepin[64], A.B. Kurepin[64], A. Kuryakin[111], S. Kushpil[97], J. Kvapil[113], M.J. Kweon[62], J.Y. Kwon[62], Y. Kwon[148], S.L. La Pointe[40], P. La Rocca[27], Y.S. Lai[81], A. Lakrathok[118], M. Lamanna[35], R. Langoy[131], K. Lapidus[35], P. Larionov[53], E. Laudi[35], L. Lautner[35], R. Lavicka[38], T. Lazareva[115], R. Lea[24], J. Lee[135], S. Lee[148], J. Lehrbach[40], R.C. Lemmon[96], I. León Monzón[122], E.D. Lesser[19], M. Lettrich[35], P. Lévai[146], X. Li[11], X.L. Li[7], J. Lien[131], R. Lietava[113], B. Lim[17], S.H. Lim[17], V. Lindenstruth[40], A. Lindner[49], C. Lippmann[109], A. Liu[19], J. Liu[129], I.M. Lofnes[21], V. Loginov[95], C. Loizides[98], P. Loncar[36], J.A. Lopez[106], X. Lopez[136], E. López Torres[8], J.R. Luhder[145], M. Lunardon[28], G. Luparello[61], Y.G. Ma[41], A. Maevskaya[64], M. Mager[35], S.M. Mahmood[20], T. Mahmoud[44], A. Maire[138], R.D. Majka[I,147], M. Malaev[100], Q.W. Malik[20], L. Malinina[IV,76], D. Mal'Kevich[94], N. Mallick[51], P. Malzacher[109], G. Mandaglio[33,57], V. Manko[90], F. Manso[136], V. Manzari[54], Y. Mao[7], M. Marchisone[137], J. Mareš[67], G.V. Margagliotti[24], A. Margotti[55], A. Marín[109], C. Markert[121], M. Marquard[69], N.A. Martin[106], P. Martinengo[35], J.L. Martinez[127], M.I. Martínez[46], G. Martínez García[117], S. Masciocchi[109], M. Masera[25], A. Masoni[56], L. Massacrier[79], A. Mastroserio[140,54], A.M. Mathis[107], O. Matonoha[82], P.F.T. Matuoka[123], A. Matyja[120], C. Mayer[120], F. Mazzaschi[25], M. Mazzilli[54], M.A. Mazzoni[59], A.F. Mechler[69], F. Meddi[22], Y. Melikyan[64], A. Menchaca-Rocha[72], C. Mengke[7], E. Meninno[116,30], A.S. Menon[127], M. Meres[13], S. Mhlanga[126], Y. Miake[135], L. Micheletti[25], L.C. Migliorin[137], D.L. Mihaylov[107], K. Mikhaylov[76,94], A.N. Mishra[146,70], D. Miśkowiec[109], A. Modak[4], N. Mohammadi[35], A.P. Mohanty[63], B. Mohanty[88], M. Mohisin Khan[16], Z. Moravcova[91], C. Mordasini[107], D.A. Moreira De Godoy[145], L.A.P. Moreno[46], I. Morozov[64], A. Morsch[35], T. Mrnjavac[35], V. Muccifora[53], E. Mudnic[36], D. Mühlheim[145], S. Muhuri[142], J.D. Mulligan[81], A. Mulliri[23,56], M.G. Munhoz[123], R.H. Munzer[69], H. Murakami[134],

S. Murray[126], L. Musa[35], J. Musinsky[65], C.J. Myers[127], J.W. Myrcha[143], B. Naik[50], R. Nair[87], B.K. Nandi[50], R. Nania[55], E. Nappi[54], M.U. Naru[14], A.F. Nassirpour[82], C. Nattrass[132], R. Nayak[50], S. Nazarenko[111], A. Neagu[20], L. Nellen[70], S.V. Nesbo[37], G. Neskovic[40], D. Nesterov[115], B.S. Nielsen[91], S. Nikolaev[90], S. Nikulin[90], V. Nikulin[100], F. Noferini[55], S. Noh[12], P. Nomokonov[76], J. Norman[129], N. Novitzky[135], P. Nowakowski[143], A. Nyanin[90], J. Nystrand[21], M. Ogino[84], A. Ohlson[82], J. Oleniacz[143], A.C. Oliveira Da Silva[132], M.H. Oliver[147], B.S. Onnerstad[128], C. Oppedisano[60], A. Ortiz Velasquez[70], T. Osako[47], A. Oskarsson[82], J. Otwinowski[120], K. Oyama[84], Y. Pachmayer[106], S. Padhan[50], D. Pagano[141], G. Paić[70], J. Pan[144], S. Panebianco[139], P. Pareek[142], J. Park[62], J.E. Parkkila[128], S. Parmar[102], S.P. Pathak[127], B. Paul[23], J. Pazzini[141], H. Pei[7], T. Peitzmann[63], X. Peng[7], L.G. Pereira[71], H. Pereira Da Costa[139], D. Peresunko[90], G.M. Perez[8], S. Perrin[139], Y. Pestov[5], V. Petráček[38], M. Petrovici[49], R.P. Pezzi[71], S. Piano[61], M. Pikna[13], P. Pillot[117], O. Pinazza[55,35], L. Pinsky[127], C. Pinto[27], S. Pisano[53], M. Płoskoń[81], M. Planinic[101], F. Pliquett[69], M.G. Poghosyan[98], B. Polichtchouk[93], N. Poljak[101], A. Pop[49], S. Porteboeuf-Houssais[136], J. Porter[81], V. Pozdniakov[76], S.K. Prasad[4], R. Preghenella[55], F. Prino[60], C.A. Pruneau[144], I. Pshenichnov[64], M. Puccio[35], S. Qiu[92], L. Quaglia[25], R.E. Quishpe[127], S. Ragoni[113], J. Rak[128], A. Rakotozafindrabe[139], L. Ramello[32], F. Rami[138], S.A.R. Ramirez[46], A.G.T. Ramos[34], R. Raniwala[104], S. Raniwala[104], S.S. Räsänen[45], R. Rath[51], I. Ravasenga[92], K.F. Read[98,132], A.R. Redelbach[40], K. Redlich[V,87], A. Rehman[21], P. Reichelt[69], F. Reidt[35], R. Renfordt[69], Z. Rescakova[39], K. Reygers[106], A. Riabov[100], V. Riabov[100], T. Richert[82,91], M. Richter[20], P. Riedler[35], W. Riegler[35], F. Riggi[27], C. Ristea[68], S.P. Rode[51], M. Rodríguez Cahuantzi[46], K. Røed[20], R. Rogalev[93], E. Rogochaya[76], T.S. Rogoschinski[69], D. Rohr[35], D. Röhrich[21], P.F. Rojas[46], P.S. Rokita[143], F. Ronchetti[53], A. Rosano[33,57], E.D. Rosas[70], A. Rossi[58], A. Rotondi[29], A. Roy[51], P. Roy[112], O.V. Rueda[82], R. Rui[24], B. Rumyantsev[76], A. Rustamov[89], E. Ryabinkin[90], Y. Ryabov[100], A. Rybicki[120], H. Rytkonen[128], O.A.M. Saarimaki[45], R. Sadek[117], S. Sadovsky[93], J. Saetre[21], K. Šafařík[38], S.K. Saha[142], S. Saha[88], B. Sahoo[50], P. Sahoo[50], R. Sahoo[51], S. Sahoo[66], D. Sahu[51], P.K. Sahu[66], J. Saini[142], S. Sakai[135], S. Sambyal[103], V. Samsonov[100,95], D. Sarkar[144], N. Sarkar[142], P. Sarma[43], V.M. Sarti[107], M.H.P. Sas[147,63], J. Schambach[98,121], H.S. Scheid[69], C. Schiaua[49], R. Schicker[106], A. Schmah[106], C. Schmidt[109], H.R. Schmidt[105], M.O. Schmidt[106], M. Schmidt[105], N.V. Schmidt[98,69], A.R. Schmier[132], J. Schukraft[35], Y. Schutz[138], K. Schwarz[109], K. Schweda[109], G. Scioli[26], E. Scomparin[60], J.E. Seger[15], Y. Sekiguchi[134], D. Sekihata[134], I. Selyuzhenkov[109,95], S. Senyukov[138], J.J. Seo[62], D. Serebryakov[64], L. Šerkšnytė[107], A. Sevcenco[68], A. Shabanov[64], A. Shabetai[117], R. Shahoyan[35], W. Shaikh[112], A. Shangaraev[93], A. Sharma[102], H. Sharma[120], M. Sharma[103], N. Sharma[102], S. Sharma[103], O. Sheibani[127], A.I. Sheikh[142], K. Shigaki[47], M. Shimomura[85], S. Shirinkin[94], Q. Shou[41], Y. Sibiriak[90], S. Siddhanta[56], T. Siemiarczuk[87], D. Silvermyr[82], G. Simatovic[92], G. Simonetti[35], B. Singh[107], R. Singh[88], R. Singh[103], R. Singh[51], V.K. Singh[142], V. Singhal[142], T. Sinha[112], B. Sitar[13], M. Sitta[32], T.B. Skaali[20], M. Slupecki[45], N. Smirnov[147], R.J.M. Snellings[63], C. Soncco[114], J. Song[127], A. Songmoolnak[118], F. Soramel[28], S. Sorensen[132], I. Sputowska[120], J. Stachel[106], I. Stan[68], P.J. Steffanic[132], S.F. Stiefelmaier[106], D. Stocco[117], M.M. Storetvedt[37], L.D. Stritto[30], C.P. Stylianidis[92], A.A.P. Suaide[123], T. Sugitate[47], C. Suire[79], M. Suljic[35], R. Sultanov[94], M. Šumbera[97], V. Sumberia[103], S. Sumowidagdo[52], S. Swain[66], A. Szabo[13], I. Szarka[13], U. Tabassam[14], S.F. Taghavi[107], G. Taillepied[136], J. Takahashi[124], G.J. Tambave[21], S. Tang[136,7], Z. Tang[130], M. Tarhini[117], M.G. Tarzila[49], A. Tauro[35], G. Tejeda Muñoz[46], A. Telesca[35], L. Terlizzi[25], C. Terrevoli[127], G. Tersimonov[3], S. Thakur[142], D. Thomas[121], F. Thoresen[91], R. Tieulent[137], A. Tikhonov[64], A.R. Timmins[127], M. Tkacik[119], A. Toia[69], N. Topilskaya[64], M. Toppi[53], F. Torales-Acosta[19], S.R. Torres[38,9], A. Trifiró[33,57], S. Tripathy[70], T. Tripathy[50], S. Trogolo[28], G. Trombetta[34], L. Tropp[39], V. Trubnikov[3], W.H. Trzaska[128], T.P. Trzcinski[143], B.A. Trzeciak[38], A. Tumkin[111], R. Turrisi[58], T.S. Tveter[20], K. Ullaland[21], E.N. Umaka[127], A. Uras[137], G.L. Usai[23], M. Vala[39], N. Valle[29], S. Vallero[60], N. van der Kolk[63], L.V.R. van Doremalen[63], M. van Leeuwen[92], P. Vande Vyvre[35], D. Varga[146], Z. Varga[146], M. Varga-Kofarago[146], A. Vargas[46], M. Vasileiou[86], A. Vasiliev[90], O. Vázquez Doce[107], V. Vechernin[115], E. Vercellin[25], S. Vergara Limón[46], L. Vermunt[63], R. Vértesi[146],

M. Verweij[63], L. Vickovic[36], Z. Vilakazi[133], O. Villalobos Baillie[113], G. Vino[54], A. Vinogradov[90], T. Virgili[30], V. Vislavicius[91], A. Vodopyanov[76], B. Volkel[35], M.A. Völkl[105], K. Voloshin[94], S.A. Voloshin[144], G. Volpe[34], B. von Haller[35], I. Vorobyev[107], D. Voscek[119], J. Vrláková[39], B. Wagner[21], M. Weber[116], A. Wegrzynek[35], S.C. Wenzel[35], J.P. Wessels[145], J. Wiechula[69], J. Wikne[20], G. Wilk[87], J. Wilkinson[109], G.A. Willems[145], E. Willsher[113], B. Windelband[106], M. Winn[139], W.E. Witt[132], J.R. Wright[121], Y. Wu[130], R. Xu[7], S. Yalcin[78], Y. Yamaguchi[47], K. Yamakawa[47], S. Yang[21], S. Yano[47,139], Z. Yin[7], H. Yokoyama[63], I.-K. Yoo[17], J.H. Yoon[62], S. Yuan[21], A. Yuncu[106], V. Yurchenko[3], V. Zaccolo[24], A. Zaman[14], C. Zampolli[35], H.J.C. Zanoli[63], N. Zardoshti[35], A. Zarochentsev[115], P. Závada[67], N. Zaviyalov[111], H. Zbroszczyk[143], M. Zhalov[100], S. Zhang[41], X. Zhang[7], Y. Zhang[130], V. Zherebchevskii[115], Y. Zhi[11], D. Zhou[7], Y. Zhou[91], J. Zhu[7,109], Y. Zhu[7], A. Zichichi[26], G. Zinovjev[3], N. Zurlo[141]

Affiliation Notes

[I] Deceased
[II] Also at: Italian National Agency for New Technologies, Energy and Sustainable Economic Development (ENEA), Bologna, Italy
[III] Also at: Dipartimento DET del Politecnico di Torino, Turin, Italy
[IV] Also at: M.V. Lomonosov Moscow State University, D.V. Skobeltsyn Institute of Nuclear, Physics, Moscow, Russia
[V] Also at: Institute of Theoretical Physics, University of Wroclaw, Poland

Collaboration Institutes

[1] A.I. Alikhanyan National Science Laboratory (Yerevan Physics Institute) Foundation, Yerevan, Armenia
[2] AGH University of Science and Technology, Cracow, Poland
[3] Bogolyubov Institute for Theoretical Physics, National Academy of Sciences of Ukraine, Kiev, Ukraine
[4] Bose Institute, Department of Physics and Centre for Astroparticle Physics and Space Science (CAPSS), Kolkata, India
[5] Budker Institute for Nuclear Physics, Novosibirsk, Russia
[6] California Polytechnic State University, San Luis Obispo, California, United States
[7] Central China Normal University, Wuhan, China
[8] Centro de Aplicaciones Tecnológicas y Desarrollo Nuclear (CEADEN), Havana, Cuba
[9] Centro de Investigación y de Estudios Avanzados (CINVESTAV), Mexico City and Mérida, Mexico
[10] Chicago State University, Chicago, Illinois, United States
[11] China Institute of Atomic Energy, Beijing, China
[12] Chungbuk National University, Cheongju, Republic of Korea
[13] Comenius University Bratislava, Faculty of Mathematics, Physics and Informatics, Bratislava, Slovakia
[14] COMSATS University Islamabad, Islamabad, Pakistan
[15] Creighton University, Omaha, Nebraska, United States
[16] Department of Physics, Aligarh Muslim University, Aligarh, India
[17] Department of Physics, Pusan National University, Pusan, Republic of Korea
[18] Department of Physics, Sejong University, Seoul, Republic of Korea
[19] Department of Physics, University of California, Berkeley, California, United States
[20] Department of Physics, University of Oslo, Oslo, Norway

[21] Department of Physics and Technology, University of Bergen, Bergen, Norway
[22] Dipartimento di Fisica dell'Università 'La Sapienza' and Sezione INFN, Rome, Italy
[23] Dipartimento di Fisica dell'Università and Sezione INFN, Cagliari, Italy
[24] Dipartimento di Fisica dell'Università and Sezione INFN, Trieste, Italy
[25] Dipartimento di Fisica dell'Università and Sezione INFN, Turin, Italy
[26] Dipartimento di Fisica e Astronomia dell'Università and Sezione INFN, Bologna, Italy
[27] Dipartimento di Fisica e Astronomia dell'Università and Sezione INFN, Catania, Italy
[28] Dipartimento di Fisica e Astronomia dell'Università and Sezione INFN, Padova, Italy
[29] Dipartimento di Fisica e Nucleare e Teorica, Università di Pavia and Sezione INFN, Pavia, Italy
[30] Dipartimento di Fisica 'E.R. Caianiello' dell'Università and Gruppo Collegato INFN, Salerno, Italy
[31] Dipartimento DISAT del Politecnico and Sezione INFN, Turin, Italy
[32] Dipartimento di Scienze e Innovazione Tecnologica dell'Università del Piemonte Orientale and INFN Sezione di Torino, Alessandria, Italy
[33] Dipartimento di Scienze MIFT, Università di Messina, Messina, Italy
[34] Dipartimento Interateneo di Fisica 'M. Merlin' and Sezione INFN, Bari, Italy
[35] European Organization for Nuclear Research (CERN), Geneva, Switzerland
[36] Faculty of Electrical Engineering, Mechanical Engineering and Naval Architecture, University of Split, Split, Croatia
[37] Faculty of Engineering and Science, Western Norway University of Applied Sciences, Bergen, Norway
[38] Faculty of Nuclear Sciences and Physical Engineering, Czech Technical University in Prague, Prague, Czech Republic
[39] Faculty of Science, P.J. Šafárik University, Košice, Slovakia
[40] Frankfurt Institute for Advanced Studies, Johann Wolfgang Goethe-Universität Frankfurt, Frankfurt, Germany
[41] Fudan University, Shanghai, China
[42] Gangneung-Wonju National University, Gangneung, Republic of Korea
[43] Gauhati University, Department of Physics, Guwahati, India
[44] Helmholtz-Institut für Strahlen- und Kernphysik, Rheinische Friedrich-Wilhelms-Universität Bonn, Bonn, Germany
[45] Helsinki Institute of Physics (HIP), Helsinki, Finland
[46] High Energy Physics Group, Universidad Autónoma de Puebla, Puebla, Mexico
[47] Hiroshima University, Hiroshima, Japan
[48] Hochschule Worms, Zentrum für Technologietransfer und Telekommunikation (ZTT), Worms, Germany
[49] Horia Hulubei National Institute of Physics and Nuclear Engineering, Bucharest, Romania
[50] Indian Institute of Technology Bombay (IIT), Mumbai, India
[51] Indian Institute of Technology Indore, Indore, India
[52] Indonesian Institute of Sciences, Jakarta, Indonesia
[53] INFN, Laboratori Nazionali di Frascati, Frascati, Italy
[54] INFN, Sezione di Bari, Bari, Italy
[55] INFN, Sezione di Bologna, Bologna, Italy
[56] INFN, Sezione di Cagliari, Cagliari, Italy
[57] INFN, Sezione di Catania, Catania, Italy
[58] INFN, Sezione di Padova, Padova, Italy
[59] INFN, Sezione di Roma, Rome, Italy
[60] INFN, Sezione di Torino, Turin, Italy
[61] INFN, Sezione di Trieste, Trieste, Italy
[62] Inha University, Incheon, Republic of Korea
[63] Institute for Gravitational and Subatomic Physics (GRASP), Utrecht University/Nikhef, Utrecht,

Netherlands
[64] Institute for Nuclear Research, Academy of Sciences, Moscow, Russia
[65] Institute of Experimental Physics, Slovak Academy of Sciences, Košice, Slovakia
[66] Institute of Physics, Homi Bhabha National Institute, Bhubaneswar, India
[67] Institute of Physics of the Czech Academy of Sciences, Prague, Czech Republic
[68] Institute of Space Science (ISS), Bucharest, Romania
[69] Institut für Kernphysik, Johann Wolfgang Goethe-Universität Frankfurt, Frankfurt, Germany
[70] Instituto de Ciencias Nucleares, Universidad Nacional Autónoma de México, Mexico City, Mexico
[71] Instituto de Física, Universidade Federal do Rio Grande do Sul (UFRGS), Porto Alegre, Brazil
[72] Instituto de Física, Universidad Nacional Autónoma de México, Mexico City, Mexico
[73] iThemba LABS, National Research Foundation, Somerset West, South Africa
[74] Jeonbuk National University, Jeonju, Republic of Korea
[75] Johann-Wolfgang-Goethe Universität Frankfurt Institut für Informatik, Fachbereich Informatik und Mathematik, Frankfurt, Germany
[76] Joint Institute for Nuclear Research (JINR), Dubna, Russia
[77] Korea Institute of Science and Technology Information, Daejeon, Republic of Korea
[78] KTO Karatay University, Konya, Turkey
[79] Laboratoire de Physique des 2 Infinis, Irène Joliot-Curie, Orsay, France
[80] Laboratoire de Physique Subatomique et de Cosmologie, Université Grenoble-Alpes, CNRS-IN2P3, Grenoble, France
[81] Lawrence Berkeley National Laboratory, Berkeley, California, United States
[82] Lund University Department of Physics, Division of Particle Physics, Lund, Sweden
[83] Moscow Institute for Physics and Technology, Moscow, Russia
[84] Nagasaki Institute of Applied Science, Nagasaki, Japan
[85] Nara Women's University (NWU), Nara, Japan
[86] National and Kapodistrian University of Athens, School of Science, Department of Physics , Athens, Greece
[87] National Centre for Nuclear Research, Warsaw, Poland
[88] National Institute of Science Education and Research, Homi Bhabha National Institute, Jatni, India
[89] National Nuclear Research Center, Baku, Azerbaijan
[90] National Research Centre Kurchatov Institute, Moscow, Russia
[91] Niels Bohr Institute, University of Copenhagen, Copenhagen, Denmark
[92] Nikhef, National institute for subatomic physics, Amsterdam, Netherlands
[93] NRC Kurchatov Institute IHEP, Protvino, Russia
[94] NRC «Kurchatov»Institute - ITEP, Moscow, Russia
[95] NRNU Moscow Engineering Physics Institute, Moscow, Russia
[96] Nuclear Physics Group, STFC Daresbury Laboratory, Daresbury, United Kingdom
[97] Nuclear Physics Institute of the Czech Academy of Sciences, Řež u Prahy, Czech Republic
[98] Oak Ridge National Laboratory, Oak Ridge, Tennessee, United States
[99] Ohio State University, Columbus, Ohio, United States
[100] Petersburg Nuclear Physics Institute, Gatchina, Russia
[101] Physics department, Faculty of science, University of Zagreb, Zagreb, Croatia
[102] Physics Department, Panjab University, Chandigarh, India
[103] Physics Department, University of Jammu, Jammu, India
[104] Physics Department, University of Rajasthan, Jaipur, India
[105] Physikalisches Institut, Eberhard-Karls-Universität Tübingen, Tübingen, Germany
[106] Physikalisches Institut, Ruprecht-Karls-Universität Heidelberg, Heidelberg, Germany
[107] Physik Department, Technische Universität München, Munich, Germany
[108] Politecnico di Bari and Sezione INFN, Bari, Italy
[109] Research Division and ExtreMe Matter Institute EMMI, GSI Helmholtzzentrum für

Schwerionenforschung GmbH, Darmstadt, Germany
[110] Rudjer Bošković Institute, Zagreb, Croatia
[111] Russian Federal Nuclear Center (VNIIEF), Sarov, Russia
[112] Saha Institute of Nuclear Physics, Homi Bhabha National Institute, Kolkata, India
[113] School of Physics and Astronomy, University of Birmingham, Birmingham, United Kingdom
[114] Sección Física, Departamento de Ciencias, Pontificia Universidad Católica del Perú, Lima, Peru
[115] St. Petersburg State University, St. Petersburg, Russia
[116] Stefan Meyer Institut für Subatomare Physik (SMI), Vienna, Austria
[117] SUBATECH, IMT Atlantique, Université de Nantes, CNRS-IN2P3, Nantes, France
[118] Suranaree University of Technology, Nakhon Ratchasima, Thailand
[119] Technical University of Košice, Košice, Slovakia
[120] The Henryk Niewodniczanski Institute of Nuclear Physics, Polish Academy of Sciences, Cracow, Poland
[121] The University of Texas at Austin, Austin, Texas, United States
[122] Universidad Autónoma de Sinaloa, Culiacán, Mexico
[123] Universidade de São Paulo (USP), São Paulo, Brazil
[124] Universidade Estadual de Campinas (UNICAMP), Campinas, Brazil
[125] Universidade Federal do ABC, Santo Andre, Brazil
[126] University of Cape Town, Cape Town, South Africa
[127] University of Houston, Houston, Texas, United States
[128] University of Jyväskylä, Jyväskylä, Finland
[129] University of Liverpool, Liverpool, United Kingdom
[130] University of Science and Technology of China, Hefei, China
[131] University of South-Eastern Norway, Tonsberg, Norway
[132] University of Tennessee, Knoxville, Tennessee, United States
[133] University of the Witwatersrand, Johannesburg, South Africa
[134] University of Tokyo, Tokyo, Japan
[135] University of Tsukuba, Tsukuba, Japan
[136] Université Clermont Auvergne, CNRS/IN2P3, LPC, Clermont-Ferrand, France
[137] Université de Lyon, CNRS/IN2P3, Institut de Physique des 2 Infinis de Lyon , Lyon, France
[138] Université de Strasbourg, CNRS, IPHC UMR 7178, F-67000 Strasbourg, France, Strasbourg, France
[139] Université Paris-Saclay Centre d'Etudes de Saclay (CEA), IRFU, Départment de Physique Nucléaire (DPhN), Saclay, France
[140] Università degli Studi di Foggia, Foggia, Italy
[141] Università di Brescia and Sezione INFN, Brescia, Italy
[142] Variable Energy Cyclotron Centre, Homi Bhabha National Institute, Kolkata, India
[143] Warsaw University of Technology, Warsaw, Poland
[144] Wayne State University, Detroit, Michigan, United States
[145] Westfälische Wilhelms-Universität Münster, Institut für Kernphysik, Münster, Germany
[146] Wigner Research Centre for Physics, Budapest, Hungary
[147] Yale University, New Haven, Connecticut, United States
[148] Yonsei University, Seoul, Republic of Korea